Title
Ferrocene-Chelating Heteroscorpionate Ligands Support Zinc Complexes as Redox Switchable Catalysts

Author
Reuter, Tate

Publication Date
2018

Peer reviewed|Thesis/dissertation

UNIVERSITY OF CALIFORNIA

Los Angeles

Ferrocene-Chelating Heteroscorpionate Ligands Support Zinc Complexes as Redox Switchable Catalysts

A thesis submitted in partial satisfaction of the

requirements for the degree Master of Science

in Chemistry

by

Tate Christopher Reuter

2018

ABSTRACT OF THE THESIS

Ferrocene-Chelating Heteroscorpionate Ligands

Support Zinc Complexes as Redox Switchable Catalysts

by

Tate Christopher Reuter

Master of Science in Chemistry

University of California, Los Angeles, 2018

Professor Paula Loredana Diaconescu, Chair

Ferrocene-chelating heteroscorpionate compounds based on [fc(PPh_2)(BH[(3-R-5-R'-1-H)$_2$pz]$_2$)] (fc = 1,1'-ferrocenediyl, pz = pyrazole) are studied and characterized for their role in the synthesis of block copolymers. The ferrocene scaffold is part of a heteroscorpionate ligand that supports late transition metals. A zinc complex, [fc(PPh_2)(BH[(3,5-Me-1H)$_2$pz]$_2$)]Zn(μ-OCH_2Ph), was synthesized previously and shown to exist in a dimeric state. Herein, the substituents on the pyrazole fragments of the scorpionate are replaced with bulkier groups to force the formation of a monomeric compound in order to arrive at a redox switchable catalyst.

The thesis of Tate Christopher Reuter is approved.

Richard B. Kaner

Ellen May Sletten

Paula Loredana Diaconescu, Committee Chair

University of California, Los Angeles

2018

This work is dedicated to my loving family and those

making a sacrifice to better themselves and the world we share.

TABLE OF CONTENTS

List of Figures

Chapter 1

Chapter 2

Nomenclature

δ	chemical shift in ppm
ppm	parts per million
NMR	nuclear magnetic resonance
TMEDA	N,N,N’,N’-tetramethylethylenediamine
TBE	1,1,2,2-tetrabromoethane
THF	tetrahydrofuran
DCM	dichloromethane
Et_2O	diethyl ether
Fc	mono substituted ferrocenyl
fc	1,1’-disubstituted ferrocenediyl
pz	pyrazole
Cp	cyclopentadienyl
Me	methyl
Ph	phenyl
Bn	benzyl
t-Bu	*tert*-butyl
LA	lactide
CL	ε-caprolactone
η	eta
$fc^{P,B}$	$fc(PPh_2)(BH[(3,5\text{-}Me)_2pz]_2)$
ROP	ring-opening polymerization

Acknowledgments

I want to thank two great mentors and friends, Kevin Swartz and Mark Abubekerov. Kevin is a wonderful person who helped me become accustomed to research lab work and, more specifically, glovebox work. Mark was pivotal in my interest and commitment to organometallic chemistry and the lab. Over the course of time I was working with Mark, I grew as a researching chemist and built a steadfast confidence in my lab skills and understanding of organometallic chemistry. I extend my sincerest thanks to both of them and wish them both the best in their endeavors.

To my advisor, Paula Diaconescu, thanks for all the opportunities and support given to me. She allowed me to apply my curiosities in chemistry in a hands-on environment that reaffirmed my interest in the field. Above all else, she was someone who was easy to talk to and helped me to do more than I had ever imagined in chemistry.

Chapter 1 - Introduction

1.1 Organometallic Chemistry and Motivations

Organometallic chemistry is, by its very name, the coupling of metals with organic compounds. It deals with the direct formation of metal-carbon bonds, which facilitate the introduction of a wide array of functional groups. With a focus on green chemistry and the well-being of our environment, organometallic chemistry offers the potential for sustainable and bio-friendly products, energy storage, and an increase the fidelity of the atom economy.[1] With this in mind, this thesis focuses on organometallic compounds and their role in catalysis, specifically, the production of novel materials, namely polymers.

1.2 Ferrocene

A unique subset of organometallic compounds are the metallocenes; these compounds share a sandwich structure with a central metal and two aromatic carbon rings on either side. Ferrocene was the first of this class to be discovered and has become ubiquitous in organometallic chemistry and transition metal chemistry.[2,3] Iron is an earth abundant and non-noble metal that makes it an economically viable commodity in chemistry. Since its finding, there have been many instances of ferrocene's application in medicine, nanotechnologies, materials, and catalysis.[4,5] While there are reports of ferrocene derivatives used as catalysts, there is a notably unique role that ferrocene can play as the scaffold that supports a catalytic center. Ferrocene has, therefore, been used in both heterogeneous and homogeneous catalysis, and displays many appealing and tunable properties that can influence the outcome of a catalytic process.

1.2.1 Structural Properties

Ferrocene is an orange solid that is stable in air and a wide array of solvents. It contains an iron center in the +2 oxidation state with two cyclopentadienyl rings on either side. The cyclopentadienyl rings each have a -1 charge and coordinate to the iron in a symmetric η^5 fashion. This negative charge, from the extra electron of the five-carbon system, gives each of the rings aromaticity and has been thoroughly studied for its reactivity and limitations.[6] The aromaticity arises from the conjugation of the p_z orbitals on the carbon atoms into the delocalized π-system and gives the rings a planar geometry. The symmetry of ferrocene has been observed to change depending on the relative orientation of the cyclopentadienyl rings. If the two rings are eclipsed, it has D_{5h} symmetry; staggered rings give rise to D_{5d} symmetry (Figure 1-1).

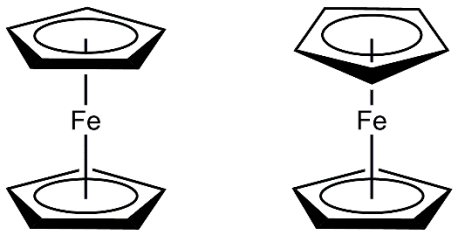

Figure 1-1. Eclipsed and staggered configurations of ferrocene

The freely rotating rings can be constrained through coordination to give ferrocene a large steric presence in a catalyst's backbone. This rigidity would easily arise from a 1,1'- disubstitution that either closes to form a metallacycle structure; or when the two ends complex with a second metal center. The symmetric 1,1'- disubstitution is the first approach and often endeavored for its synthetic simplicity, however, there could also be an asymmetric approach to functionalizing the two rings individually. In changing the symmetry of the pre-catalyst, the influence of monomer

incorporation into the growing polymer chain is altered as well. The way the coordination sphere is oriented can be directly correlated to the tacticity the eventual polymer chain will obtain.

In this vein, considerations are taken towards the likely polymeric tacticity that can be achieved. This is realized through the active symmetry of the catalyst, whereby varying catalyst symmetries gives rise to distinct enantioselectivities and tacticities during polymerization.[7] An example of this is an *ansa*-zirconocene catalyst used in propylene polymerizations. This catalyst has C_2 symmetry, this allows for directed monomer incorporation and results in the formation of isotactic polypropylene (Figure 1-2).[8] Similarly, these *ansa*-zirconocene catalysts with C_s symmetry have been reported to afford syndiotactic polymers.

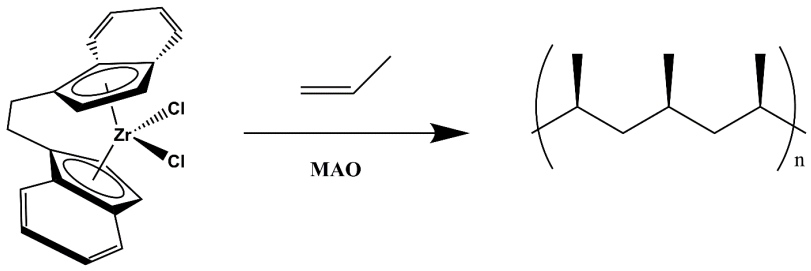

Figure 1-2. Polymerization of propylene by a C_2 symmetric *ansa*-zirconocene catalyst; MAO is methylaluminoxane and acts as a coinitiator

A careful consideration needs to be made when modifying the ferrocene rings; a loss of aromaticity may be induced upon manipulating the ferrocene structure. For this reason, the handling of ferrocene derivatives and subsequent complexes is done under an inert atmosphere to maintain the integrity of the corresponding samples and circumvent their decomposition.

1.2.2 Electronic and Redox Properties

Unmodified ferrocene is diamagnetic and has an 18 electron count. Deriving the molecular orbital diagram, one would find that the electrons fill the bonding orbitals completely and none of the anti-bonding, further supporting the enhanced stability of ferrocene. This gives the compound an opportunity for electronic tuning, because the stability will support adjustments to the cyclopentadienyl rings while modulating the electron density around the iron center. This facet of ferrocene makes it ideal when coupled to a second metal as the catalytic center. Tunability of the ligands will produce changes in the electron communication from ferrocene to the catalytic center that could prove crucial in monomer selectivity and incorporation. This communication could arise from electron withdrawing/donating effects of the substituents, conjugation, or proximity of the second metal. At an extreme, the iron center can interact directly with the other metal center. Our group explored these interactions; Figure 1-3 shows the corresponding frontier molecular orbitals.[9]

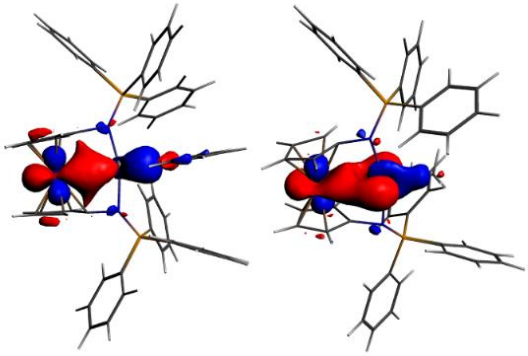

Figure 1-3. Frontier molecular orbitals: HOMO−6 for $[fc(NPPh_3)_2NiPh]^+$ (left) and HOMO−4 for $[fc(NPPh_3)_2PdMe]^+$ (right); isosurface value = 0.03.

Reprinted with permission from *Organometallics*, **2017**, 36 (22), pp 4394–4402. Copyright 2017 American Chemical Society.[9]

The interaction between the ferrocene iron and nickel or palladium affects the phosphine-metal lability. The metal-metal interaction described above was used as motive for the inapplicability of those specific nickel and palladium compounds in redox switchable chemistry. The electrochemical experiments pointed towards either an irreversible oxidation or complete redox inactivity. The nickel compound and similar heteroscorpionate nickel compounds have been unsuccessful in polymerization. A heteroscorpionate palladium compound has been reported for a norborene polymerization only. With this information, and discussed later herein, attention was given to zinc as the catalytic metal.

Along with its stability, ferrocene is capable of fast and well-behaved electron transfers and has the ability to exist in two distinct oxidation states. Either through direct chemical or electrochemical methods, ferrocene has been observed in the +2 and the +3 oxidation state (Figure 1-4).

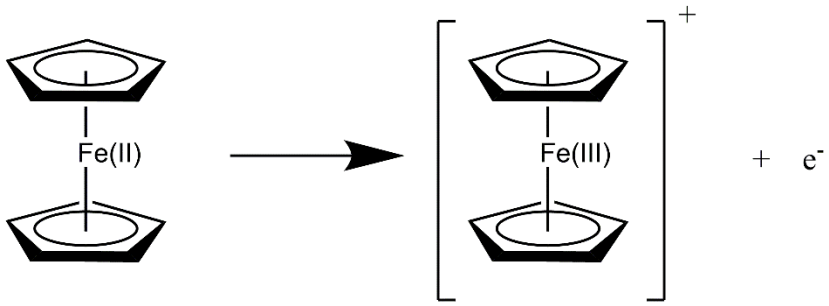

Figure 1-4. A general oxidation of ferrocene

A low oxidation potential is an attractive feature for a ferrocene backbone in catalysis. An important factor of the redox potential is how the ligand modifications will change this potential, therefore, one would need to consider the influence of specific functional groups on the redox potential. Work has been done by Silva *et al.* to determine how substitution to the aromatic rings alters the redox potentials.[10] A consequence of the high stability of ferrocene is that large changes

to the redox potential are not observed and therefore need not be considered too delicately when determining how drastic the modifications would affect redox behavior. The main appeal for redox active catalysts is the ability to turn the catalyst 'on' and 'off.' Reports have shown that through this oxidation, one can modulate the substrate incorporation at a single catalytic site for polymerization.[12] To expand further, there is potential to have one catalyst act selectively depending on the oxidation state of the ferrocene. This offers a route to one-pot procedures where the orthogonal reactivity of a catalyst in a given oxidation state will produce a polymer of desired substrate; changing the oxidation state changes substrate incorporation. This further offers the opportunity for block copolymerizations; examples have been demonstrated by our group as well as others.[12, 13] Figure 1-5 shows an example of how this is realized.[14]

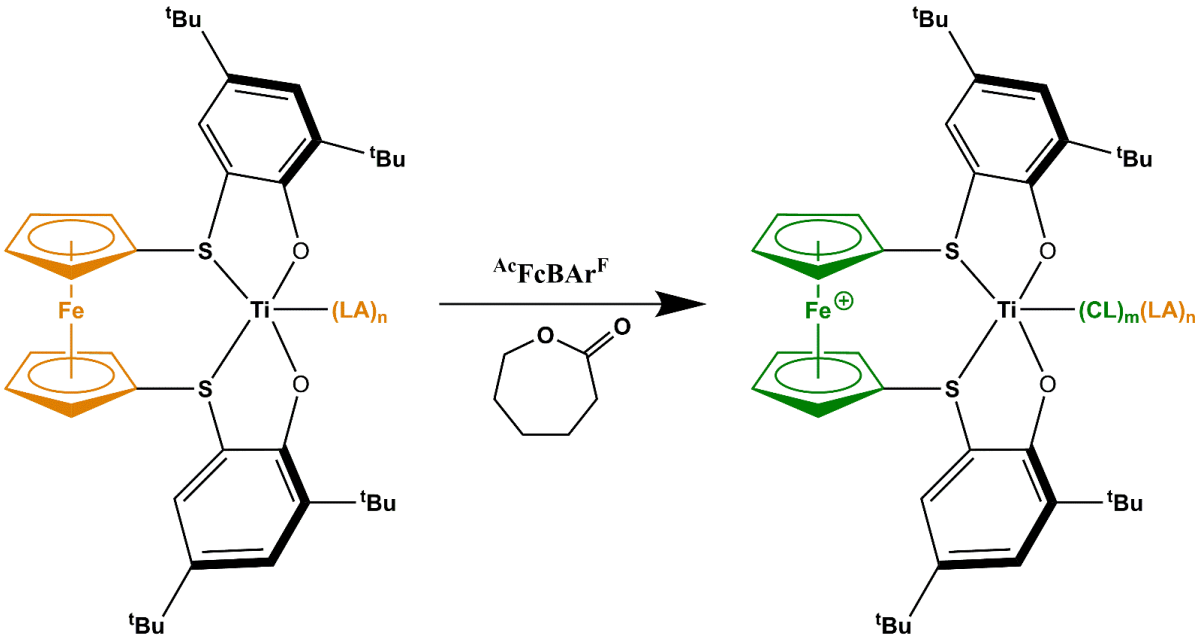

Figure 1-5. Chemical oxidation of a ferrocene supported titanium complex facilitates the block copolymerization of lactide and ε-caprolactone

Chapter 2 – Ferrocene-Chelating Heteroscorpionate Ligands

2.1 Poly(pyrazolyl)borates

Probing appropriate ligands that can afford both electronic and steric tunability of a metal complex, consideration is given to poly(pyrazolyl)borates. This class of compounds is often referred to as "scorpionates" and since its origin has developed a reputation in catalytic chemistry.[15-17] These scorpionate ligands are composed of pyrazole fragments that bear two adjacent nitrogens and three carbons to form a five-membered ring. The ring has opportunity for substitutions to be made on any one or two or all three of the carbons (Figure 2-1). This variability is what affords the compound such tunability for both steric and electronic properties. The 1-position on the pyrazole can contain other organic fragments, but here the nitrogen bears a hydrogen that is cleaved during the formation of the scorpionate and so it is not altered.

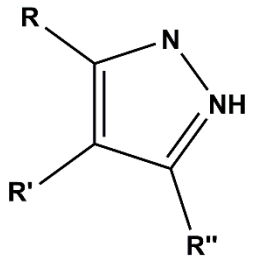

Figure 2-1. A generic 3-R-4-R'-5-R"-1H-pyrazol that can be tuned for catalytic optimization. The R groups can all be the same or different to attain the desired ligand effect.

To form the poly(pyrazolyl)borate, the desired pyrazolyl fragments are attached to the boron center and then the sought after scorpionate is afforded; the name of this compound is derived from the scorpion-type attack and coordination it displays with a metal. A representation of the 'scorpion' can be seen in Figure 2-2(a). If all three coordination sites to the metal are the same, it is characterized as a homoscorpionate, Figure 2-2(b).

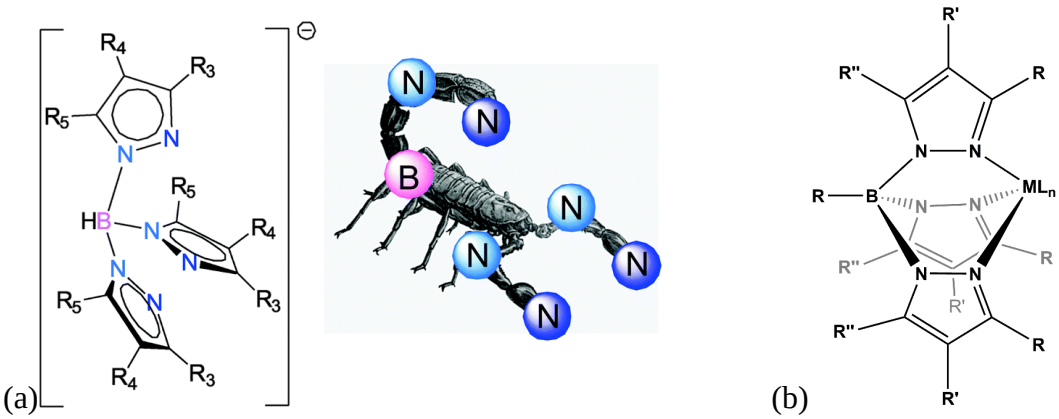

Figure 2-2. (a) A comparison of the scorpionate ligand to its likeness of a scorpion; (b) A generic homoscorpionate structure; L are generic ligands.

Figure 2-2(a) was Reprinted with permission from *Phys. Chem. Chem. Phys.*, **2014**, 16, 14514-14522. Copyright 2014 PCCP.[18]

This chelation affords the scorpionate a reputation in coordination chemistry and has been seen in multiple catalytic processes.[19-26] An exploitable feature of this scorpionate is its redox inactivity, which makes it a prime substituent for the redox active ferrocene. By incorporating the redox activity of ferrocene with these redox inactive moieties, progress is made towards honing in on a ligand design with one distinct redox event. The coordination of poly(pyrazolyl)borates is a field that has been studied and known ferrocene derivatives with this appendage are reported in the literature.[27-32] A few examples can be seen in Figure 2-3.

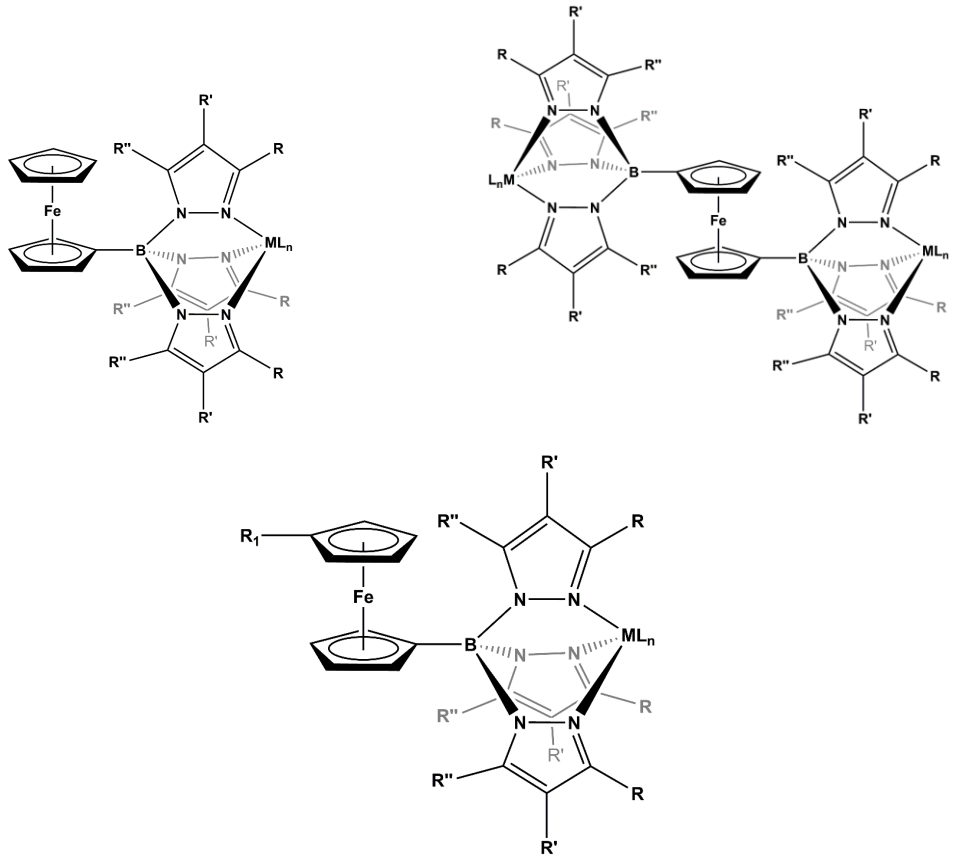

Figure 2-3. Examples of possible poly(pyrazolyl)borate appended ferrocene derivatives

In the bottom example of Figure 2-3 there is opportunity for adding a second, different fragment to that ferrocene derivative, thereby making a heteroscorpionate ligand. Utilizing the chelation of the pyrazole fragments and the incorporation of another chelating group in the R_1 position in the same figure, further modification to the electronic and steric properties of the pro-ligand can be realized.

2.2 Phosphine Groups

Phosphines are groups that behave well with surrounding redox activity and have the ability to coordinate to metals. Examples of phosphines being used in organometallic catalysis can be seen in numerous derivatives of Grubbs work as well as others.[33] The position of the phosphine allows for a metal-phosphine interaction to occur. Depending on the substituents of the phosphine, one could potentially modulate how strong or weak that interaction is. This is due to the bonding and subsequent back-bonding that is displayed by the phosphine and metal respectively. The bulkiness of the ligand can also be modified by changing the appended group, thus further adding rigidity to the compound (Figure 2-4). During catalysis, the phosphine group does not necessarily participate, but often is used for its lability.

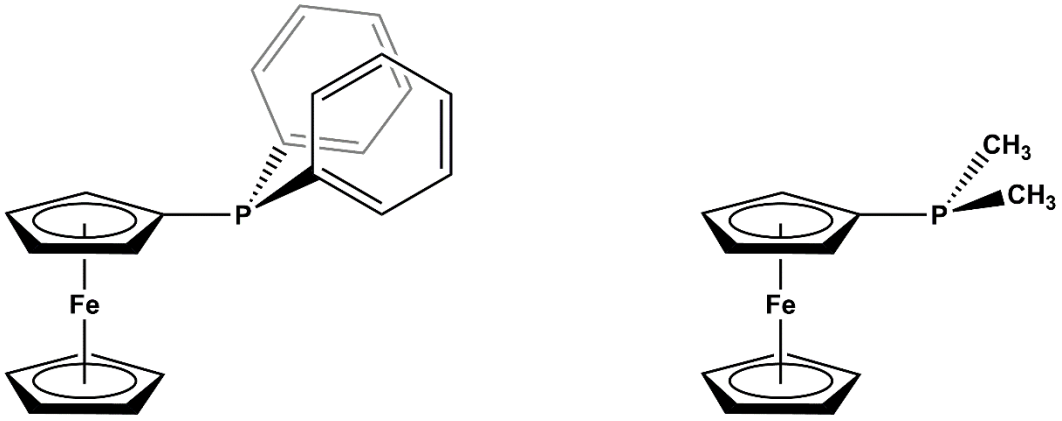

Figure 2-4. Demonstrating the effect that the phosphine group could have on the steric presence of the pro-ligand (angled to account for metal chelation)

The ability of the phosphine to actively associate and dissociate from the metal center allows for monomer incorporation during catalysis.[34] Examples in the literature can be found that show the existence of ferrocene derivatives bearing a phosphine.[35] Variations of these types are shown in Figure 2-5.

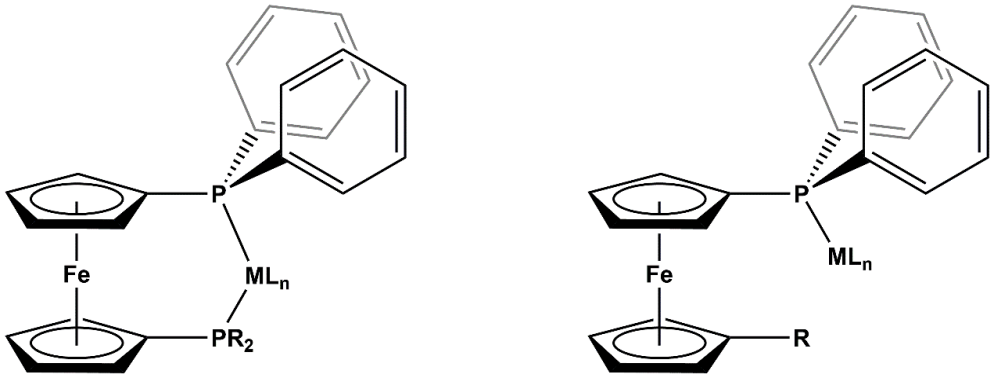

Figure 2-5. Two examples of observed phosphine coordination

2.3 Results and Discussion

The ferrocene starting material first underwent a lithiation reaction, whose product is stabilized by a TMEDA chelate, to afford two cyclopentadienyl rings that were substituted in a symmetric 1,1'- fashion (Figure 2-6). This procedure is well known and followed from the literature.[37]

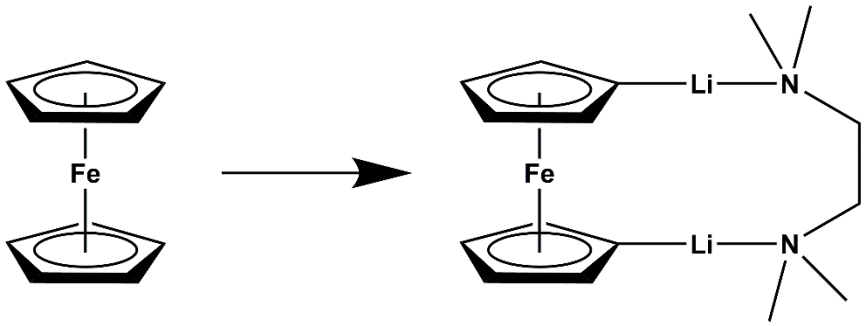

Figure 2-6. Synthesis of 1,1'-dilithioferrocene – $fc(Li)_2(TMEDA)$

In order to arrive at a compound robust enough to undergo a further modification, a bromination reaction followed. This reaction has been reported in literature, but deviations to the original procedure were made.[38] The differences include stirring at a low temperature for only two hours instead of the reported six, and stirring at ambient temperature for 16 hours instead of the reported 10. The 1,1'-dibromoferrocene was isolated in excellent yields (Figure 2-7). The major side product, easily screened by NMR spectroscopy, is the mono-bromo ferrocene impurity (a result of incomplete bromination). Using short recrystallization intervals of a maximum of four hours, most of this impurity, as well as others, can be washed away.

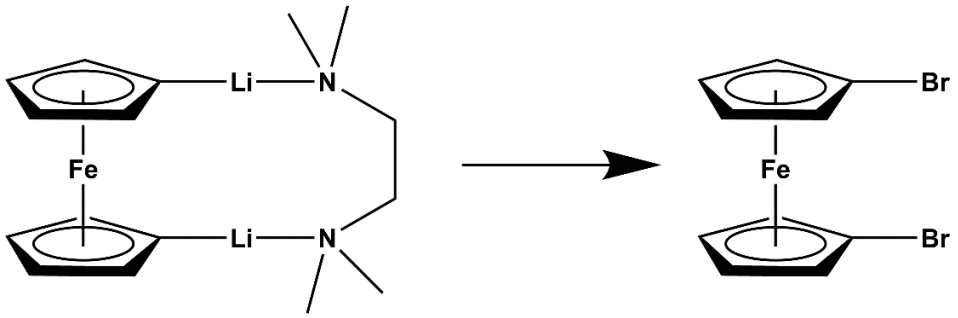

Figure 2-7. Synthesis of 1,1'-dibromoferrocene – $fcBr_2$

With the dibromo compound synthesized, the appendage of the phosphine group was the next modification. The procedure for this step was adapted from the literature.[39] The difference comes in the purification through flash column chromatography over dry silica: the solvent system was switched from petroleum ether and diethyl ether to petroleum ether and dichloromethane. This change in the solvent system allows for a greater separation on the gel than before, producing a significantly cleaner desired product, 1'-bromo-1-diphenylphosphinoferrocene (Figure 2-8). The main side-product observed is 1,1'-di(diphenylphosphino)ferrocene, in which both Cp-bromine bonds were cleaved.

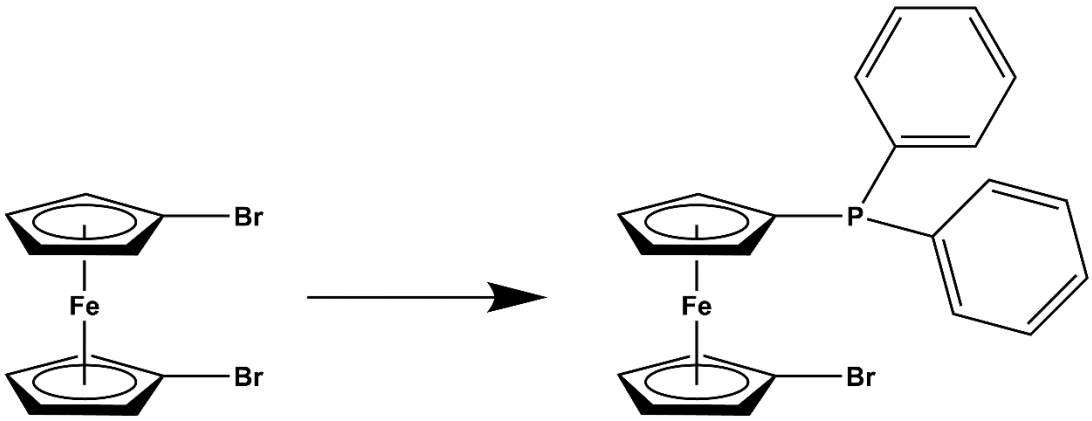

Figure 2-8. Synthesis of 1'-bromo-1-diphenylphosphinoferrocene – $fcBr(PPh_2)$

With the desired intermediate, 1'-bromo-1-diphenylphosphinoferrocene in hand, a borylation reaction was carried out to replace bromine in order to add the boron center required for the formation of the pyrazolyl borate. This was achieved using the highly reactive *n*-butyl lithium to cleave the bromine. This was a deviation from the reported procedure that requires the addition of all reagents at once.[40] By separating the lithiation and the borylation steps, an intermediate can be obtained and purified. This allows for higher compound purity and full conversion in both reactions. Once the lithiation reaction is complete (Figure 2-9), the rapid addition of a borate can yield the asymmetrically substituted ferrocene with a boron center (Figure 2-10).

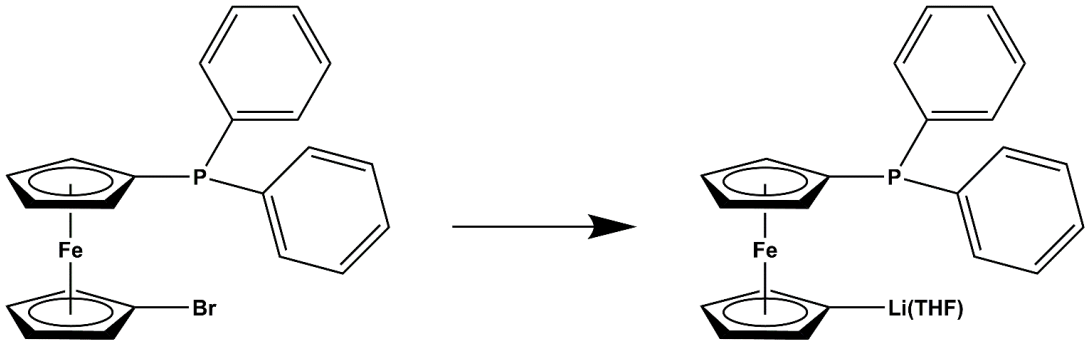

Figure 2-9. Synthesis of 1'-lithio-1-diphenylphosphinoferrocene – [fc(PPh_2)Li][THF]

The rapid addition of the borate is crucial to the success of this reaction. There is a notable green tinge that can be observed on the outset while the solution stirs when this procedure is carried out properly. For example, a slow addition does not display this coloration and often concludes with poor yields.

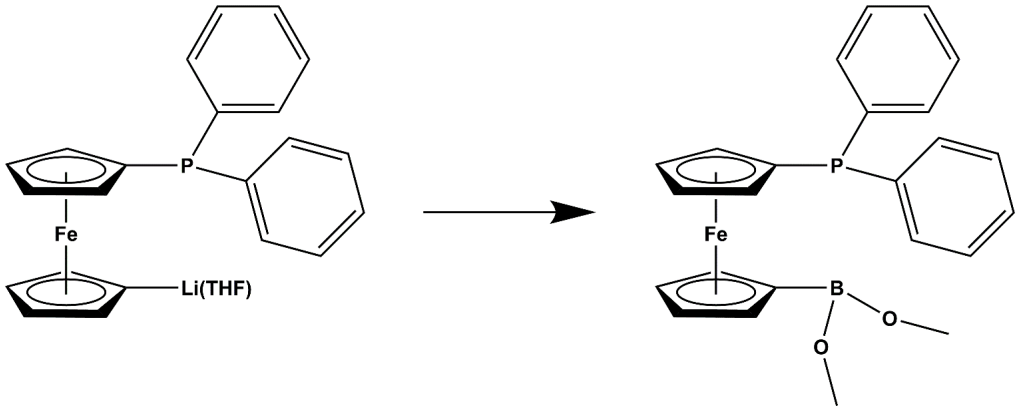

Figure 2-10. Synthesis of 1'-dimethoxyborate-1-diphenylphosphinoferrocene – fc(PPh_2)(B[$OMe]_2$)

The formation of pyrazolyl borates is often accomplished with the use of reactive borohydride species. To obtain such a compound, the borate of the synthesized 1'-dimethoxyborate-1-diphenylphosphinoferrocene was reduced with lithium aluminum hydride to afford the borohydride species. This compound is stabilized by a lithium salt that coordinates solvent, as demonstrated by the corresponding NMR spectra. This lithium salt provides a means to perform pyrazolyl borate chemistry at temperatures far reduced from traditional synthetic methods (Figure 2-11).

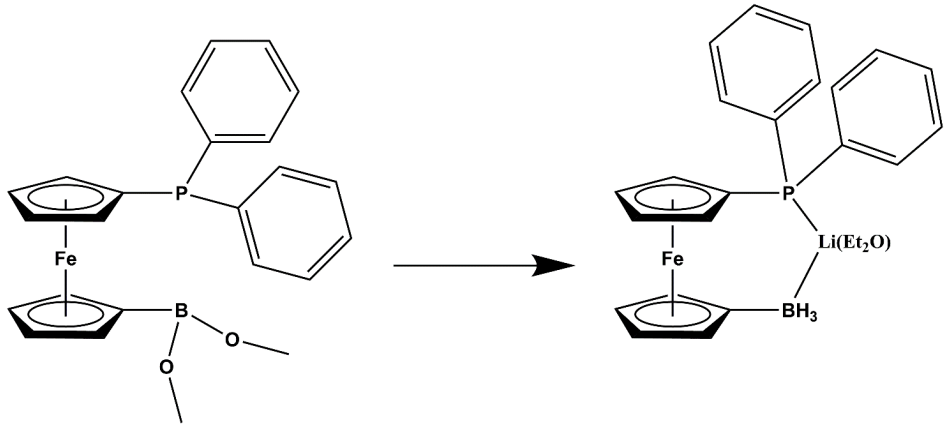

Figure 2-11. Synthesis of [fc(PPh_2)(BH_3)][Li(OEt_2)]

To obtain the heteroscorpionate pro-ligand, temperatures as low as 50 °C were used for its successful formation. A drawback, however, when using these lithium salts is their decomposition due to lithium dissociation even at not too high temperatures. Control experiments (see Appendix) show that at elevated temperatures, beyond the boiling point of the solvent coordinated to the lithium, the compound will begin to decompose and lose the boron attachment. Another hindrance is the reagent exactness required for the success of the following reactions. The current synthetic approach does not allow the use of an excess of pyrazole due to the difficulty in separating it from the pro-ligand. This means that a careful set-up and monitoring of this reaction are required to assure complete formation of $[fc(PPh_2)(BH[(3,5\text{-}Me)_2pz]_2)][Li(THF)_2]$ is achieved and no excess pyrazole remains. As an additional note, it is more favorable to carry through some unreacted compound than an excess of pyrazole. With these considerations, the pro-ligand was successfully synthesized and characterized (Figure 2-12).

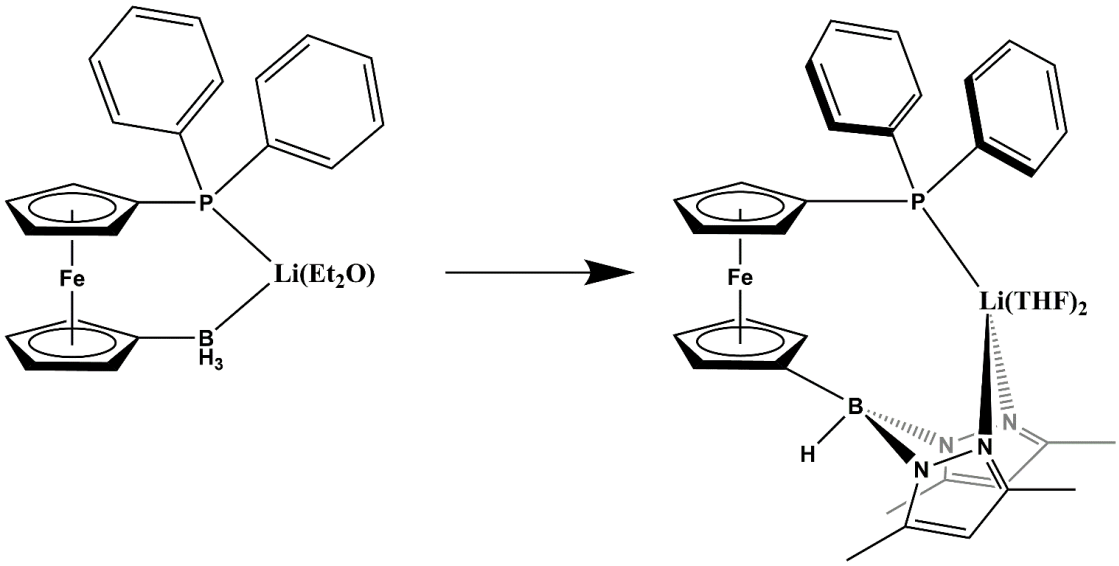

Figure 2-12. Synthesis of $[fc(PPh_2)(BH[(3,5\text{-}Me)_2pz]_2)][Li(THF)_2]$ - $fc^{P,B}[Li(THF)^2]$

The original goal of the project discussed herein was to force the formation of a monomeric catalytic species. This goal was established because a zinc complex supported by a dimethyl

derivative of the pyrazolyl borate discussed above is an active catalyst for the polymerization of cyclic esters but its dimeric form does not allow for a differentiation in reactivity between the corresponding reduced and oxidized species. A possible approach is using larger alkyl groups on the pyrazolyl fragments. The first attempt was to employ the asymmetric 3-phenyl-5-methyl-1H-pyrazole. This pyrazole was synthesized according to the literature.[41] However, many side products are generated. The NMR spectrum of the mixture (see Appendix) shows peaks with broad bases and small peaks that suggest impurities. Literature investigations indicated that there is a tautomerization that occurs with this asymmetric pyrazole.[48] What is observed in the reaction mixture is most likely a mixture of four products; the major tautomer in solution is the desired 3-phenyl-5-methyl-1H-pyrazole, but the formation of 5-phenyl-3-methyl-1H-pyrazole means that with two pyrazolyl fragments per ligand, there are four possible products. Even though the spectrum did not indicate a pure product, the crude product of [fc(PPh_2)(BH[(3-Ph-5-Me)$_2$pz]$_2$)][Li(THF)$_2$] was used in a reaction with $ZnCl_2$ to probe the formation of a zinc species. However, similar to the prior step, it was not possible to obtain a pure product; several purification attempts were unsuccessful.

While the asymmetric pyrazole has presented a synthetic difficulty, there are alternate methods to stabilize and append the pyrazole that are currently being explored.

To exploit a relatively simple synthetic approach, the symmetric 3,5-di-*t*-butyl-1H-pyrazole was synthesized according to the literature.[42] This pyrazole was added in similar fashion to the original dimethyl derivative (see Figure 2-12 and corresponding discussion), but required an elevated temperature to achieve successful formation. This reaction was also only completed on an NMR tube scale. Attempts at scaling it up have been unsuccessful thus far. It appears that the compound decomposes before full formation is complete. What has been tried is a step-wise

increase in heat, as it was thought that the addition of one pyrazolyl fragment would increase the thermal stability of the mono(pyrazolyl) borate intermediate and allow for a jump in temperature. This too has been unsuccessful. Therefore, the formation of [fc(PPh_2)(BH[(3,5-*t*-$Bu)_2pz]_2$)][$Li(THF)_2$] has been accomplished only on a small scale (Figure 2-13).

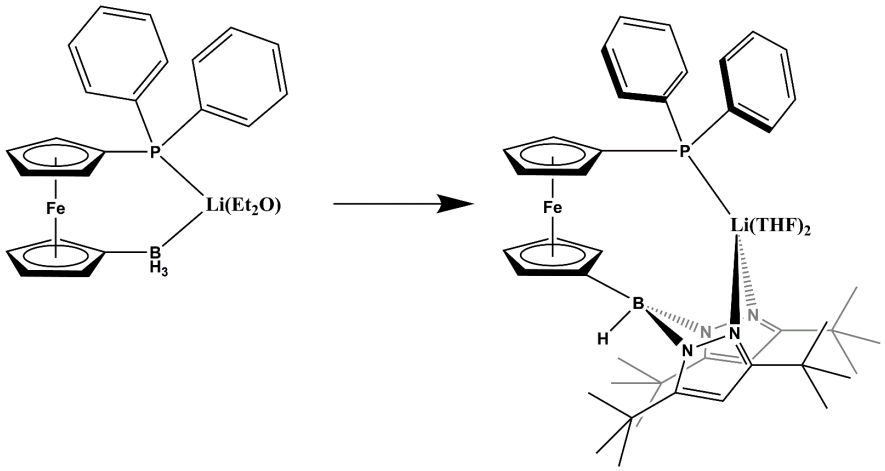

Figure 2-13. Synthesis of [fc(PPh_2)(BH[(3,5-*t*-$Bu)_2pz]_2$)][$Li(THF)_2$]

2.4 Synthesis of the Heteroscorpionate Pro-ligand [fc(PPh_2)(BH[(3,5-$Me)_2$pz]$_2$)][Li(THF)$_2$]

The synthesis of the dimethyl derivative was carried out for use in polymerization reactions. The dimethyl pyrazole was selected for its availability and simple symmetric structure. The successful synthesis of the pro-ligand depended on mild reaction conditions and the slow, controlled rates of reaction. For these reasons, and because of unwanted kinetic side-products that result at higher temperatures, the use of lowered temperatures and step-wise procedures, diverging from the literature, were employed to ensure high yields and purity. The support of the aforementioned lithium salt, observed in [fc(PPh_2)(BH_3)][Li(OEt_2)] and the following compound, relied on these lowered temperatures. This was crucial during the pyrazolyl addition reactions (Figure 2-12) and proved to be a challenge in the formation of pyrazolyl borates with larger alkyl groups. Common synthetic practices require molten or a refluxing pyrazole as the reaction medium for poly(pyrazolyl) borate synthesis, but the lithium salt offers a route to lowered activation barriers and less harsh reaction conditions. Even with the stabilizing salt, careful and precise temperature control needs to be employed for the successful synthesis of the more sterically encumbered pyrazolyl borates.

An aryl phosphine was chosen for its soft ligand type properties as it might dissociate from zinc during catalysis. This attribute is desirable in catalytic chemistry as the dissociation of the phosphine donor would expose a coordination site for the substrate to interact with the catalyst; for a polymerization reaction, for example, the polymeric chain and the monomer need to be coordinated to the metal center to allow for chain growth of the polymer. With the aforementioned considerations on ligand substitutions in mind, the successful synthesis of a heteroscorpionate pro-ligand, [fc(PPh_2)(BH[(3,5-$Me)_2$pz]$_2$)][Li(THF)$_2$], was achieved.

2.4.1 General Considerations

All procedures were performed in an MBraun Glovebox (O_2 and H_2O at < 1ppm) or on a Schlenk line using appropriate techniques unless otherwise noted. All glassware was heated to a minimum of 425 K in an oven before transfer into the drybox. All solvents were purified using the method described by Grubbs[36] or distilled from appropriate drying agents and stored under nitrogen prior to transfer into the drybox. NMR solvents obtained from Cambridge Isotope Laboratories were degassed prior to box entry and stored over activated molecular sieves. All NMR spectra were recorded on Bruker AV300 or DRX500 at ambient temperature unless noted otherwise. Proton shifts are given relative to the residual solvent peaks. Reagents were obtained from commercial vendors and used as received.

2.4.2 Successful Preparation of Pro-ligand

Synthesis[37] of 1,1'-dilithioferrocene – $fc(Li)_2$(TMEDA)

Ferrocene (10.05 g, 54.01 mmol) and TMEDA (7.53g, 64.80mmol) were added to 75 mL of hexanes. A 2.60 M solution of *n*-butyl lithium (45.70 mL, 118.81 mmol) in hexanes was added dropwise to the stirring solution. The solution was stirred over a period of 16 hours. The solution was filtered through a glass frit, and the solids collected. Volatiles were removed under a reduced pressure (13.26 g, 78%).

Synthesis[38] of 1,1'-dibromoferrocene – $fcBr_2$

$fc(Li)_2$(TMEDA) (13.26 g, 42.26 mmol) was dissolved in 100 mL of diethyl ether. 1,1,2,2-Tetrabromoethane (32.84 g, 94.74 mmol) was added to an addition funnel and the sealed apparatus was removed from the drybox. The solution was stirred at -78 °C for 30 minutes, at which point

the addition funnel was opened and allowed to add dropwise, still submerged at -78 °C. After all TBE was added, the solution was stirred at -78 °C for another 90 minutes. The solution was then stirred at ambient temperature for 16 hours. The resulting solution was quenched with 150 mL of H_2O and stirred for 30 minutes. A separatory funnel was used to extract the organic layer, washing the aqueous with diethyl ether (3x), collecting the organic fractions. The combined organic fractions were dried over $MgSO_4$ and filtered. Rotary evaporation followed by recrystallization at -40 °C from methanol afforded an orange solid (14.13 g, 96%). ^{1}H NMR (300 MHz, $CDCl_3$) δ (ppm) 4.16 (t, 4H, Cp-H, J = 1.86 Hz), 4.42 (t, 4H, Cp-H, J = 1.86 Hz); a small singlet at 1.54 ppm attributed to residual water in benchtop $CDCl_3$; small shoulder at 4.18 ppm and a singlet at 3.50 ppm were attributed to mono-bromo ferrocene.

Synthesis[39] of 1'-bromo-1-diphenylphosphinoferrocene – fcBr(PPh_2)

$fcBr_2$ (8.07 g, 23.46 mmol) was dissolved in 100 mL of THF and stirred in a cold well at -78 °C for 60 minutes. A 2.50 M solution of *n*-butyl lithium (9.38 mL, 23.46 mmol) was added dropwise to the solution and left in the cold well for an additional 15 minutes. Chlorodiphenylphosphine (5.69 g, 25.80 mmol) was diluted with THF and prepared in an addition funnel, and allowed to add dropwise. The resulting solution was stirred for another 15 minutes in the cold well, followed by 90 minutes at ambient temperature. The flask was removed from the drybox and the solution was quenched with 100 mL of H_2O. Extraction with 100 mL of dichloromethane, and washes (2x) of the aqueous layer, were collected, combined, and dried over $MgSO_4$. Filtration and rotary evaporation afforded an oily orange solid. Purification via flash column chromatography (9 : 1 :: Petroleum Ether : dichloromethane) over dry silica and recrystallization at -40 °C from diethyl ether layered with hexanes afforded a dark orange solid

(7.60 g, 72%). ^{1}H NMR (500 MHz, $CDCl_3$) δ (ppm) 3.98 (s, 2H, Cp-H), 4.15 (s, 2H, Cp-H), 4.31 (s, 2H, Cp-H), 4.42 (s, 2H, Cp-H), 7.35 (m, 10H, aromatic); singlet at 1.54 ppm was attributed to residual water in benchtop $CDCl_3$.

Synthesis[40] of 1'-lithio-1-diphenylphosphinoferrocene – [fc(PPh_2)Li][THF]

fcBr(PPh_2) (3.50 g, 7.79 mmol) was dissolved in diethyl ether / THF (50 mL / 3 mL) and stirred in a cold well at -78 °C for 60 minutes. A 2.50 M solution of *n*-butyl lithium (3.12 mL, 7.79 mmol) was added dropwise to the solution and left in the cold well for an additional 60 minutes. The solution was filtered over a glass frit and solids were washed with hexanes. The resulting orange solid was dried under a reduced pressure (2.98 g, 86%).

Synthesis[40] of 1'-dimethoxyborate-1-diphenylphosphinoferrocene – fc(PPh_2)(B[OMe]$_2$)

[fc(PPh_2)Li][THF] (1.49 g, 3.35 mmol) was dissolved in 100 mL of THF and stirred in a cold well at -78 °C for 60 minutes. A syringe loaded with trimethoxyborate (1.85 mL, 16.62 mmol) was rapidly evacuated into the solution and allowed to stir at ambient temperature for 90 minutes. Volatiles were removed under a reduced pressure. The resulting oil was dissolved in a minimal amount of toluene and filtered through a Celite plug and volatiles were removed under a reduced pressure, affording a yellow solid (1.20 g, 80%).

Synthesis[40] of [fc(PPh_2)(BH_3)][Li(OEt_2)]

fc(PPh_2)(B[OMe]$_2$) (2.40 g, 5.20 mmol) was dissolved in 100 mL of Et_2O and stirred at -78 °C in a cold well for 45 minutes. Lithium aluminum hydride (0.20 g, 5.20 mmol) in 8 mL of diethyl ether was added dropwise over a 5 minute period and stirred at -78 °C for 30 minutes

followed by stirring at ambient temperature for 60 minutes. The slurry was filtered through a glass frit and volatiles were removed under reduced pressure. The orange solid was dissolved in THF and concentrated under a reduced pressure. A volume equivalent layering of diethyl ether and cooling to -40 °C for 16 hours afforded orange solids (2.58 g, 77%). ^{1}H NMR (500 MHz, C_6D_6) δ (ppm) 4.22 (t, 4H, Cp-H, J = 1.83 Hz), 4.35 (s, 2H, Cp-H), 4.45 (s, 2H, Cp-H), 7.09 (m, 6H, *m*-Ph, *p*-Ph), 7.69 (m, 4H, *o*-Ph); peaks at 1.40 and 3.61 were attributed to coordinated and residual diethyl ether.

Synthesis[40] of [fc(PPh_2)(BH[(3,5-Me)$_2$pz]$_2$)][Li(THF)$_2$] - fc^{P,B}[Li(THF)^2]

[fc(PPh_2)(BH_3)][Li(OEt_2)] (0.52 g, 0.85 mmol) and 3,5-dimethylpyrazole (0.16 g, 1.71 mmol) were combined and dissolved in a solution of 5 mL of toluene and 1 mL of THF. The solution was heated to 50 °C for 20 hours. Volatiles were then removed under a reduced pressure. The oily solids were dissolved in minimal diethyl ether and filtered through a Celite plug, volatiles were removed under a reduced pressure affording an orange solid (0.59 g, 86%). ^{1}H NMR (300 MHz, C_6D_6) δ (ppm) 2.07 (s, 6H, -CH_3), 2.57 (s, 6H, -CH_3), 4.00 (t, 2H, Cp-H, J = 1.34 Hz), 4.08 (t, 2H, Cp-H, J = 1.55 Hz), 4.18 (t, 2H, Cp-H, J = 1.56 Hz), 4.39 (t, 2H, Cp-H, J = 1.84 Hz), 5.86 (s, 2H, -CH-), 7.04 (m, 6H, *m*-Ph, *p*-Ph), 7.56 (m, 4H, *o*-Ph); peaks at 1.29 and 3.45 were attributed to residual diethyl ether.

2.4.3 Preparation of Pyrazole

Synthesis[41] of 3-phenyl-5-methyl-1H-pyrazole

Carried out under a flow of nitrogen, 1-benzoylacetone (5.13 g, 31.6 mmol) was dissolved in 30 mL of methanol and cooled to 0 °C. Hydrazine (4.96 mL, 158 mmol) was added dropwise and stirred for 60 minutes at 0 °C. Rotary evaporation produced white solids, washing with hexanes and further rotary evaporation afforded the white solid product (4.66 g, 93%). ^{1}H NMR (300 MHz, $CDCl_3$) δ (ppm) 2.32 (s, 3H, -CH_3), 6.34 (s, 1H, -CH-), 7.31 (m, 3H, *m*-Ph, *p*-Ph), 7.70 (d, 2H, *o*-Ph, J = 7.46 Hz).

Synthesis[42] of 3,5-di-*tert*-butyl-1H-pyrazole

Carried out under a flow of nitrogen, 2,2,6,6-tetramethylheptane-3,5-dione (0.50 mL, 2.00 mmol) and hydrazine (0.098 mL, 2.00 mmol) were combined and stirred at 70 °C for 90 minutes. A white solid precipitated, was collected and washed with hexanes, and volatiles were removed under a reduced pressure to afford the white solid product (0.31 g, 92%). ^{1}H NMR (300 MHz, $CDCl_3$) δ (ppm) 1.32 (s, 18H, -CH_3), 5.89 (s, 1H, -CH-).

2.4.4 Successful Preparation of Pro-ligand with a Different Pyrazole

Synthesis of [fc(PPh_2)(BH[(3,5-*t*-Bu)$_2$pz]$_2$)][Li(THF)$_2$] -- (small scale)

3,5-di-*tert*-butyl-1H-pyrazole (3.00 mg, 0.017 mmol) and [fc(PPh_2)(BH_3)][Li(OEt_2)] (5.1 mg, 0.0084mmol) was added to 1.50 mL of C_6D_6. The tube was placed at 60 °C for twelve hours. Then the temperature was increased to 70 °C. Heating continued for an additional 16 hours until complete product formation was observed.

2.4.5 Attempted Pro-ligand Synthesis

In an attempt to block the dimerization of the zinc complex discussed herein, a substitution was tried on the pyrazolyl fragments. Specifically, a substitution at the 3- position from a methyl to a phenyl group to form an asymmetric pyrazole. No clean compound could be recovered and the NMR's were busy and hinted at multiple products. Though an attempt at pushing the crude compound through to a zinc addition was tried, no compound could be isolated. NMR spectra are available in the Appendix.

Attempted Synthesis of [fc(PPh_2)(BH[(3-Ph-5-Me)$_2$pz]$_2$)][Li(THF)$_2$]

[fc(PPh_2)(BH_3)][Li(OEt_2)] (0.53g, 0.88mmol) and 3-phenyl-5-methylpyrazole (0.28g, 1.78mmol) were combined and dissolved in a solution of 5 mL of toluene and 1 mL of THF. The solution was heated to 50 °C for 20 hours. Volatiles were then removed under a reduced pressure. The oily solids were dissolved in minimal diethyl ether and filtered through a Celite plug, volatiles were removed under a reduced pressure affording a dark orange oil. Repeated trituration and reduced pressure offered little improvement. Nonetheless, this mixture was used in the following experiment.

Attempted Synthesis of [fc(PPh_2)(BH[(3-Ph-5-Me)$_2$pz]$_2$)][$ZnCl_2$]

The product from the aforementioned experiment (72.20 mg, 0.057 mmol) in 1 mL of THF was added dropwise to $ZnCl_2$ dissolved in 2 mL of THF. The solution was stirred at ambient temperature for 120 minutes, at which point the volatiles were removed under a reduced pressure. The solids were dissolved in 10 mL of toluene and concentrated under a reduced pressure. Recrystallization at -40 °C afforded a white-orange solid. Further attempts to wash and or filtration of the product were futile, no product collected.

Chapter 3 – Zinc Complexes Supported by Ferrocene-Chelating Heteroscorpionate Ligands

3.1 Zinc

Zinc is a choice metal for biologically benign catalysts that offers low toxicity, is cheap and abundant, and has been observed to behave nicely in homogeneous catalysis.[43] Catalytic zinc centers have been employed in the catalysis for lactone and epoxide ring-opening polymerizations.[44] Due to its redox inactivity, zinc could afford a catalyst that, when coupled with ferrocene, should give rise to only one distinct redox event upon oxidation and subsequent reduction.

3.2 Results and Discussion

The synthesis of the zinc-chloride complex, [fc(PPh_2)(BH[(3,5-$Me)_2pz]_2$)]ZnCl, was previously reported and achieved here (Figure 3-1).[40]

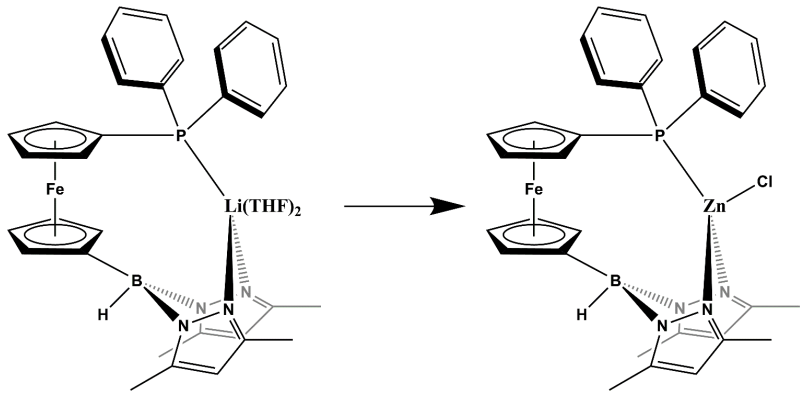

Figure 3-1. Synthesis of ($fc^{P,B}$)ZnCl

The alkoxide complex, [[fc(PPh_2)(BH[(3,5-Me-1H)$_2$pz]$_2$)]Zn(μ-OCH_2Ph)]$_2$ was also synthesized and prepared for future polymerizations (Figure 3-2).[45]

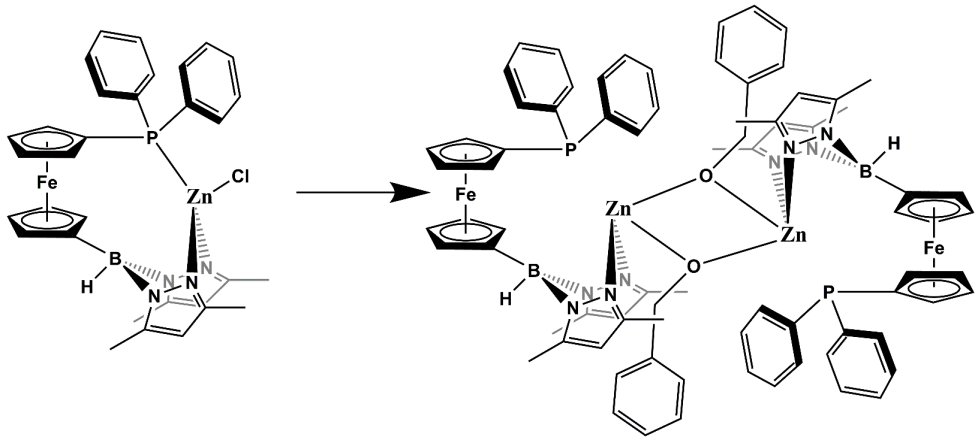

Figure 3-2. Synthesis of $[(fc^{P,B})Zn(\mu\text{-}OCH_2Ph)]_2$

There were no deviations from the reported procedures. As shown in Figure 3-2, the phosphine group no longer interacts with the zinc metal. This is attributed to the zincs highly oxophilic nature and the soft ligand properties of the aryl phosphine. The Cp-ring with the phosphine is now free to rotate around and accommodate an incoming substrate for polymerizations. An analogue of the catalytic complex, $(fc^{P,B})ZnMe$, underwent cyclic voltammetry and exhibits a single redox event (Figure 3-3). The pre-catalyst that is used, $[(fc^{P,B})Zn(\mu\text{-}OCH_2Ph)]_2$, was oxidized with $[^{Ac}Fc][BAr^F]$ (acetyl ferrocenium tetrakis(3,5-bis(trifluoromethyl)phenyl)borate) and the polymerizations in the next chapter were carried out using this oxidized form of the catalyst.

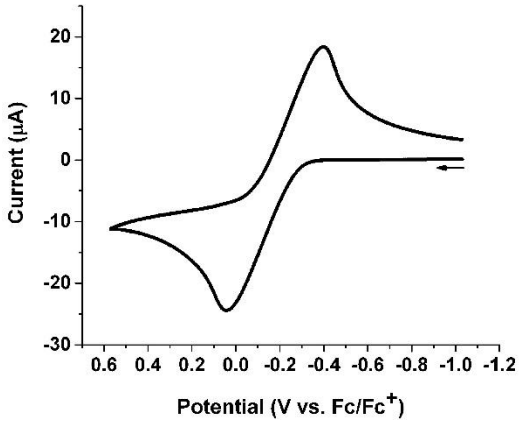

Figure 3-3. Cyclic voltammogram recorded with a glassy carbon electrode at 100 mV/s in THF, 0.10 M [TBA][PF_6] containing 5.0 mM ($fc^{P,B}$)ZnMe

Reprinted with permission from *Inorganic Chemistry*, **2015**. 54(4), pp.1778-1784. Copyright 2015 American Chemical Society.[40]

3.3 Synthesis of the Zinc Benzoxide Complex

Zinc chloride was the metal source and the pro-ligand was added very slowly at reduced temperatures to circumvent the zinc acting as a bridge for two ligands and other side-products. The alkoxide group was chosen to compliment the zincs oxophilic nature. The benzoxide was prepared *in situ* to afford the final pre-catalytic compound.

3.3.1 General Considerations

All procedures were performed in an MBraun Glovebox (O_2 and H_2O at < 1ppm) or on a Schlenk line using appropriate techniques unless otherwise noted. All glassware was heated to a minimum of 425K in an oven before transfer into the drybox. All solvents were purified using the method described by Grubbs[36] or distilled from appropriate drying agents and stored under nitrogen prior to transfer into the drybox. NMR solvents obtained from Cambridge Isotope Laboratories were degassed prior to box entry and stored over activated molecular sieves. All NMR spectra were recorded on Bruker AV300 or DRX500 at ambient temperature unless noted otherwise. Proton shifts are given relative to the residual solvent peaks. Reagents were obtained from commercial vendors and used as received.

3.3.2 Preparation of Pre-catalyst

Synthesis[40] of ($fc^{P,B}$)ZnCl

[$fc(PPh_2)(BH[(3,5\text{-}Me)_2pz]_2)$][$Li(THF)_2$] (0.59 g, 0.82 mmol) in 3 mL of THF was added dropwise to $ZnCl_2$ dissolved in 2 mL of THF. The solution was stirred at ambient temperature for 120 minutes, at which point volatiles were removed under a reduced pressure. The solids were dissolved in 10 mL of toluene and concentrated under a reduced pressure. Recrystallization at -40 °C afforded an orange solid (0.41 g, 74%). ^{1}H NMR (300 MHz, C_6D_6) δ (ppm) 2.24 (s, 6H, -CH_3), 2.47 (s, 6H, -CH_3), 3.55 (t, 2H, Cp-H, 1.65 Hz), 3.93 (s, 4H, Cp-H), 4.03 (t, 2H, Cp-H, 1.79 Hz), 5.68 (s, 2H, -CH-), 7.00 (m, 6H, *m*-Ph, *p*-Ph), 7.86 (m, 4H, *o*-Ph); excess peaks are due to residual toluene.

Synthesis[45] of [($fc^{P,B}$)Zn(μ-OCH_2Ph)]$_2$

$HOCH_2Ph$ (0.048 mL, 0.46 mmol) was added dropwise to a solution of KCH_2Ph (59.90 mg, 0.46 mmol) in 5 mL of THF at -78 °C until the solution became colorless. ($fc^{P,B}$)ZnCl (316.40 mg, 0.41 mmol) was dissolved in 2 mL of THF and added dropwise to the solution and stirred at -78 °C for 60 minutes. The solution was warmed to ambient temperature and volatiles were removed under a reduced pressure. The crude was dissolved in 5 mL of toluene and filtered through a Celite plug. Toluene was removed under a reduced pressure and the oily solids redissolved in 5 mL of diethyl ether. Prolonged standing afforded solids in the solution. Diethyl ether washes (3x) afforded a yellow-orange solid (205.30 mg, 61%). ^{1}H NMR (500 MHz, C_6D_6) δ (ppm) 2.00 (s, 6H, -CH_3), 2.47 (s, 6H, -CH_3), 3.74 (t, 2H, Cp-H, J = 1.46 Hz), 3.91 (t, 2H, Cp-H, J = 1.24 Hz), 4.03 (s, 2H, -OCH_2Ph), 4.13 (t, 2H, Cp-H, J = 1.32 Hz), 4.31 (t, 2H, Cp-H, J = 1.27 Hz), 4.89 (s, 1H, BH), 5.75 (s, 2H, -CH-), 6.70 (m, 2H, *o*-Ph), 6.81 (m, 2H, *m*-Ph), 6.86 (m, 2H, *p*-Ph), 7.04 (m, 6H, *m*-Ph, *p*-Ph), 7.54 (m, 4H, *o*-Ph); residual diethyl ether and THF give rise to remaining peaks.

Chapter 4 - Polymerization

4.1 Monomer Scope

Biodegradable polymers are composed such that upon decomposition they break down into naturally occurring products. The scope of this catalyst studied so far is in relation to polyesters. The ester bonds allows for a hydrolysis event that can break down the material back into monomeric form, and from there further decomposition to small compounds such as gaseous CO_2, water, and consolidation with biomass are possible. Examples of monomers and a polymeric product can be seen in Figure 4-1.

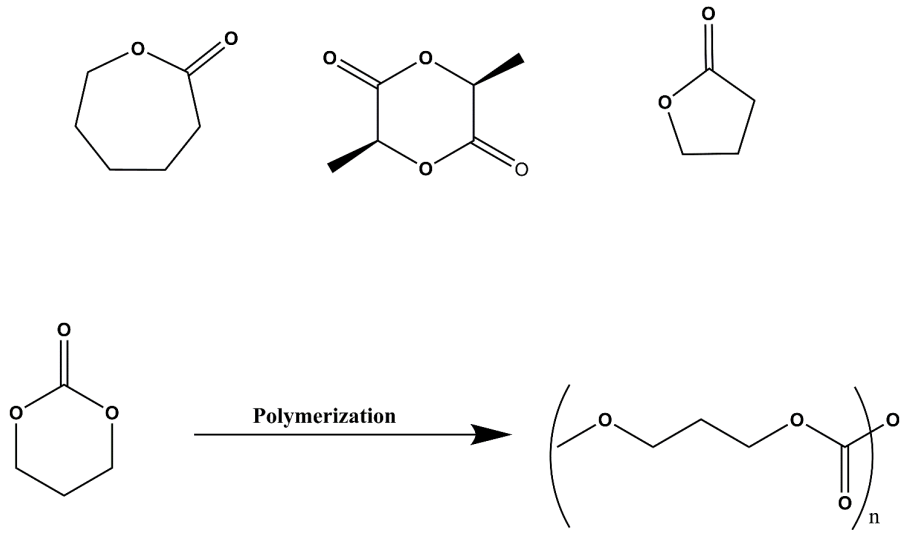

Figure 4-1. Drawings of ε-caprolactone, L-lactide, and γ-butyrolactone used as monomers (top, in order); the polymerization of trimethylene carbonate (bottom)

The pre-catalyst prepared would coordinate the substrate and undergo a ring-opening polymerization. This polymerization would afford a material that contains a number of bonds susceptible to a controlled degradation, namely the ester bond. It is this bond that is exploited for its possible decomposition. The monomer could have a variety of substitutions that offer soft and

hard polymers. If these monomers are used in block copolymerization, the modulation of hard and soft blocks could give rise to novel materials with unique and desired properties. To fully understand the use of a monomer and its environmental impact, Figure 4-2 provides insight into the lactide lifecycle.

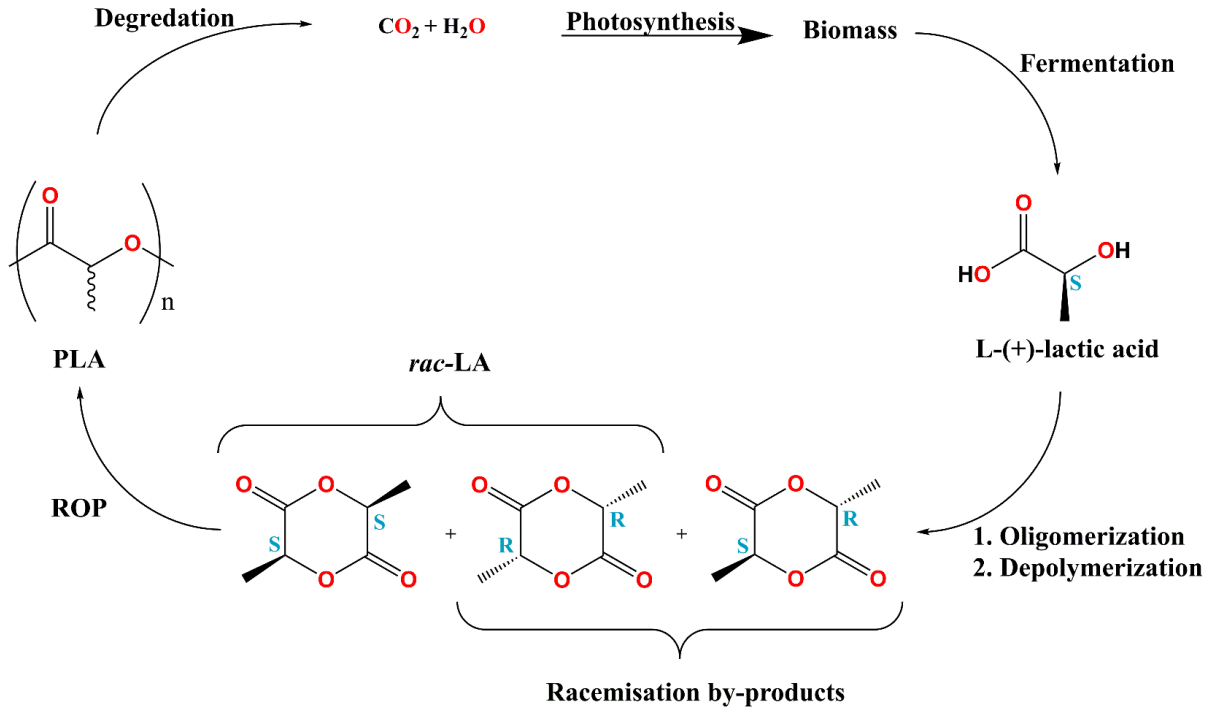

Figure 4-2. Lifecycle of lactide.[46]

4.2 Dimeric Catalyst

The current zinc alkoxide complex has been used in catalysis and multiblock copolymerization. The challenge is that the compound currently exists as a dimer, Figure 4-3.

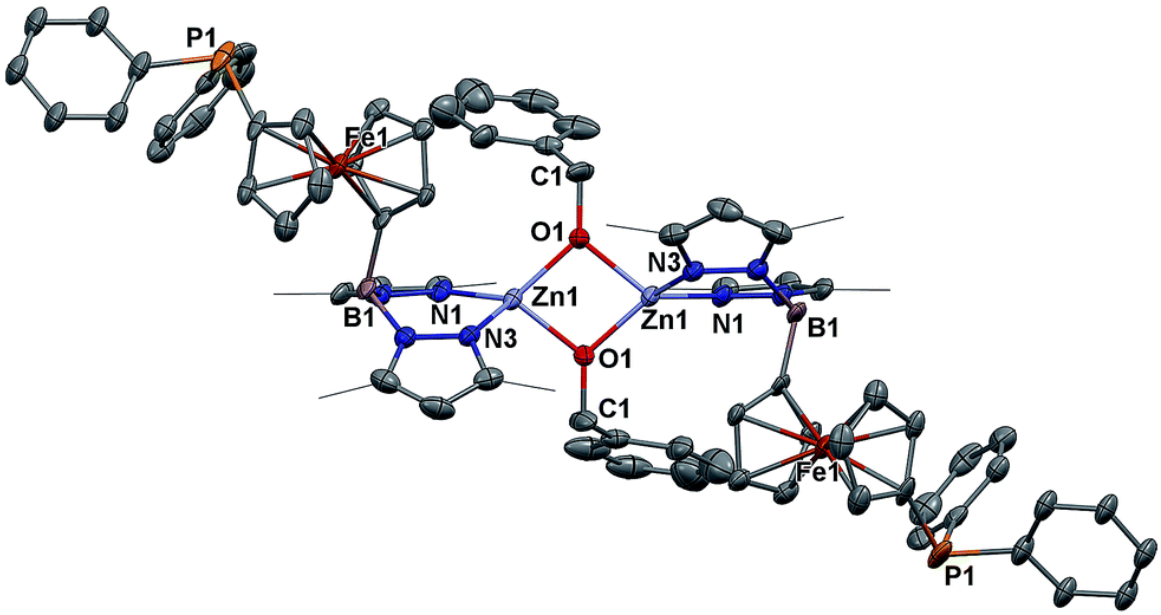

Figure 4-3. Molecular structure drawing of $[(fc^{P,B})Zn(\mu\text{-}OCH_2Ph)]_2$ with thermal ellipsoids at 50% probability; hydrogen atoms and disordered counterparts are omitted for clarity. Reprinted with permission from *Chem. Sci*., **2018**, 9, 2168-2178. Copyright 2018 Royal Chemistry Society.[45]

It is this dimeric state that prompted the need for a larger steric hindrance, this is why the work here is concerned with the influence of the pyrazolyl presence. In dissociating the dimeric compound, it is possible that the catalyst could show preferential substrate coordination through redox switching. With a monomeric species, there is also the possibility that the oxophilic zinc would display a zinc-phosphine interaction that will be more prevalent and owe more to selectivity

and communication between the ligand and zinc center. So far the dimeric catalyst has been reported for trimethylene carbonate and L-lactide copolymerization.[45]

4.3 Sugar Oligomerization

Current work is being done in a collaboration project that uses the described dimeric catalyst for an epoxide ring-opening polymerization. The goal of the project is the synthesis of a novel polymeric material as well as to study the multiple methods of sugar polymerization, be it anionic, cationic, or coordination based. The epoxidation of tri-*O*-benzyl-glucal to form 1,2-anhydro-3,4,6-tri-*O*-benzyl-α-d-glucopyranose was achieved before polymerization (Figure 4-4).

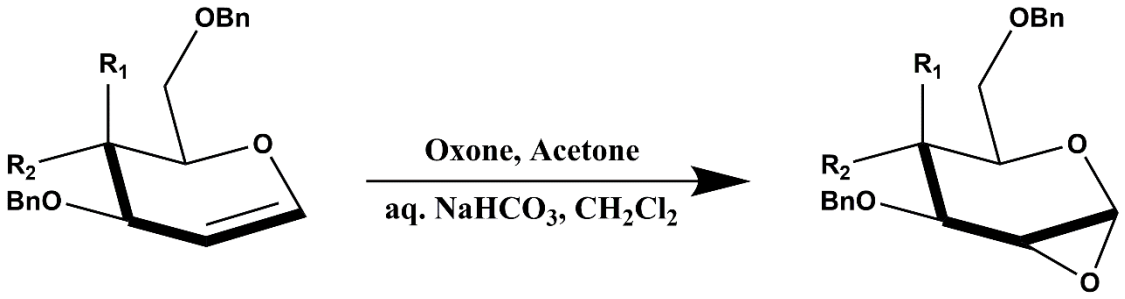

Figure 4-4. Epoxidation of tri-*O*-benzyl-glucal to afford the substrate 1,2-anhydro-3,4,6-tri-*O*-benzyl-α-d-glucopyranose. R^1 = H/OBn ; R^2 = OBn/H

The successful oligomerization of 1,2-anhydro-3,4,6-tri-*O*-benzyl-α-d-glucopyranose was carried out with an average of 14 units per chain (Figure 4-5). Though the complete characterization is still in progress, Figure 4-5 shows a likely oligomeric structure. As a note, the benzoxy group at the bottom of the oligomer in the same figure is the one obtained from the initiating group on the discussed catalyst. The use of sugar substrates for polymerization offers a route to synthetic polysaccharides that can be substituted and modulated to afford novel and desirable properties to

act as a replacement for current industry plastics and elastomers. Polysaccharides also offer an environmentally benign structure that can be broken down into naturally occurring compounds.

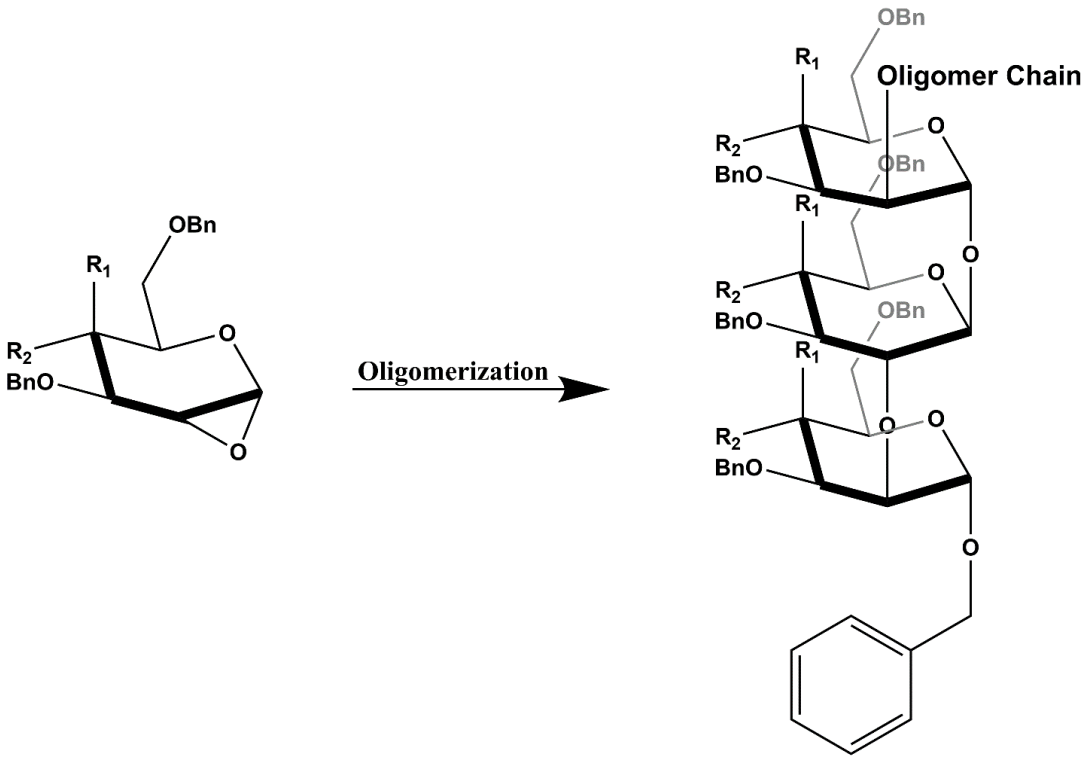

Figure 4-5. Possible structure of the carried out oligomerization of 1,2-anhydro-3,4,6-tri-*O*-benzyl-α-d-glucopyranose. R^1 = H/OBn ; R^2 = OBn/H

4.3.1 Experimental

Synthesis[47] of 1,2-anhydro-3,4,6-tri-O-benzyl-α-d-glucopyranose

5 mL DCM, 0.5 mL acetone, and 8 mL saturated $NaHCO_3$ solution are combined with 475 mg of tri-*O*-benzyl, and cooled to 0 °C, stirring vigorously. Dissolved oxone in 6 mL H_2O was added dropwise over a 20min period. Once the addition is complete, the solution was stirred at 0 °C for another 30 minutes. It was then removed from the ice-bath and continued to stir at ambient temperature. TLC was used to check the reaction progress, and if needed, more oxone (solid) and acetone were added as needed. More $NaHCO_3$ (solid) was added periodically to maintain a basic pH. Once the reaction was complete, a separatory funnel was used to extract the organic layer, washing the aqueous twice with DCM. The combined organic fractions were dried with $MgSO_4$, filtered, and the volatiles were removed under a reduced pressure. **A w**hite solid was obtained (0.344g, 68%).

Oligomerization of 1,2-anhydro-3,4,6-tri-O-benzyl-α-d-glucopyranose

4.6 mg of ($fc^{P,B}$), 6.1 mg of [^{Ac}Fc][BAr^F], and 200 mg of the monomer were added to a J-young tube with 0.5 mL of deuterated benzene and heated to 70°C for 2 hours. The solution was diluted with DCM and precipitated in 10 mL of methanol. Centrifugation and additional methanol washes afforded a dark orange polymeric product (PDI: 1.57, M_w: 6006kDa).

Chapter 5 – Conclusions and Outlook

Compound $[(fc^{P,B})Zn(\mu\text{-}OCH_2Ph)]_2$ was used previously for the copolymerization of trimethylene carbonate and lactide and it showed good activity.[45] Therefore, the synthesis of $[(fc^{P,B})Zn(\mu\text{-}OCH_2Ph)]_2$ was accomplished and the compound was used to catalyze the epoxide ring-opening polymerization of the sugar 1,2-anhydro-3,4,6-tri-O-benzyl-α-d-glucopyranose to afford a novel oligomeric material. Although the catalyst is dimeric, it is able to form biodegradable block copolymers and sugar oligomers through ring opening and epoxide ring opening polymerizations, respectively. Attempts to synthesizing a monomeric analogue of the active species through modulation of the pyrazolyl group size are discussed herein. The approach of substituting the pyrazolyl fragments asymmetrically offer challenges in overcoming the solvent facilitated tautomerization. Methods were explored that offer possible synthetic routes to achieving the successful incorporation of the asymmetric derivative. These routes include adding a stabilizing agent to allow the proper tautomer to be appended and using an excess of pyrazole with further work up to isolate the pro-ligand from excess pyrazole. The approach of synthetic simplicity through the symmetrically substituted di-*t*-butylpyrazole showed more progress than the aforementioned asymmetric approaches. The current setback is the thermal instability of the compound that conflicts with the necessity of elevated temperatures to attach the bulky pyrazole. Current investigations are focusing on adding a chelating agent to stabilize the lithium salt at these elevated temperatures. The current reaction medium for the pyrazolyl addition is primarily THF, so the possibility of forming an azeotrope as the reaction mixture is also being investigated as it could withstand higher temperatures and aid in the lithium salt stabilization.

A drawback of the dimeric catalyst is the lack of selectivity towards various substrates. This lack of specificity requires the sequential addition of monomers during block

copolymerizations. This defeats the idea of one-pot redox switchable catalysis. This lack of specificity could be a consequence of the dissociation of the phosphine donor from zinc interaction. The dimeric catalyst shows no interaction with the phosphine groups, but, instead, the oxophilic zinc centers interact only with their respective pyrazolyl groups and the shared alkoxides. Forcing a monomeric species through imposing steric hindrance could show a crucial interaction between the zinc and phosphine group. Our current hypothesis is that the presence of this interaction will allow specificity towards substrate incorporation depending on the catalyst's oxidation state. It is this redox switching that is desired when it is accompanied by preferential substrate incorporation. To achieve this goal, the successful synthesis of a bulky pro-ligand needs to be pursued. With the aforementioned approaches, a redox switchable catalyst that exists in the monomeric state is realistic and attainable.

Appendix – NMR Spectra

$fcBr_2$

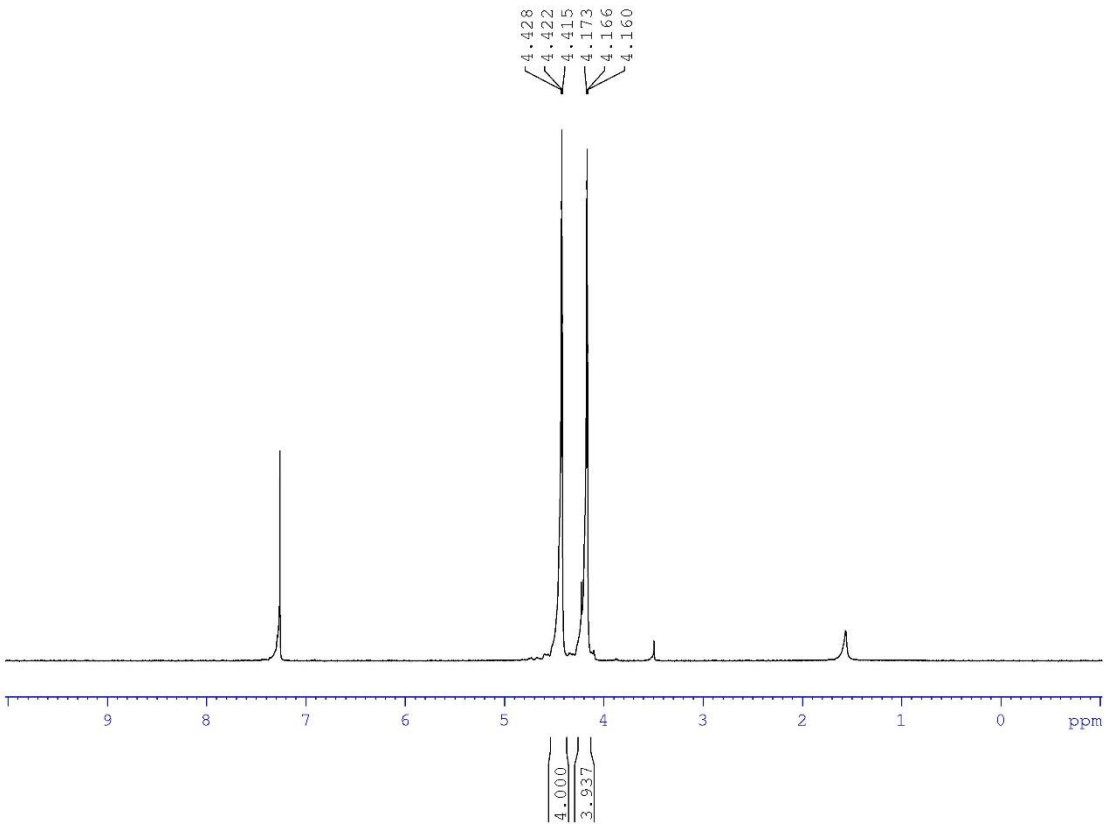

^{1}H NMR (300 MHz, $CDCl_3$) δ (ppm) 4.16 (t, 4H, Cp-H, J = 1.86 Hz), 4.42 (t, 4H, Cp-H, J = 1.86 Hz); a small singlet at 1.54 ppm was attributed to residual water in benchtop $CDCl_3$; a small shoulder at 4.18 ppm and singlet at 3.50 ppm were attributed to mono-bromo ferrocene.

fcBr(PPh_2)

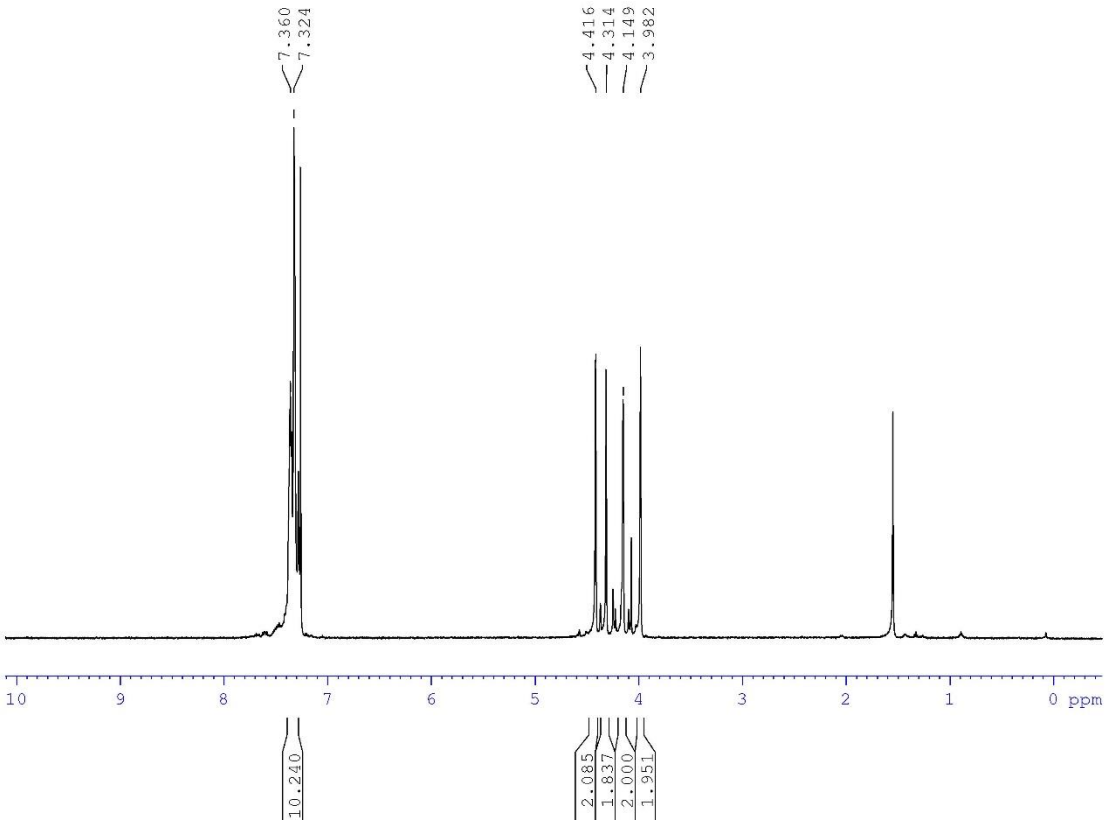

^{1}H NMR (500 MHz, $CDCl_3$) δ (ppm) 3.98 (s, 2H, Cp-H), 4.15 (s, 2H, Cp-H), 4.31 (s, 2H, Cp-H), 4.42 (s, 2H, Cp-H), 7.35 (m, 10H, aromatic); singlet at 1.54 ppm attributed to residual water in benchtop $CDCl_3$.

[fc(PPh$_2$)(BH$_3$)][Li(OEt$_2$)]

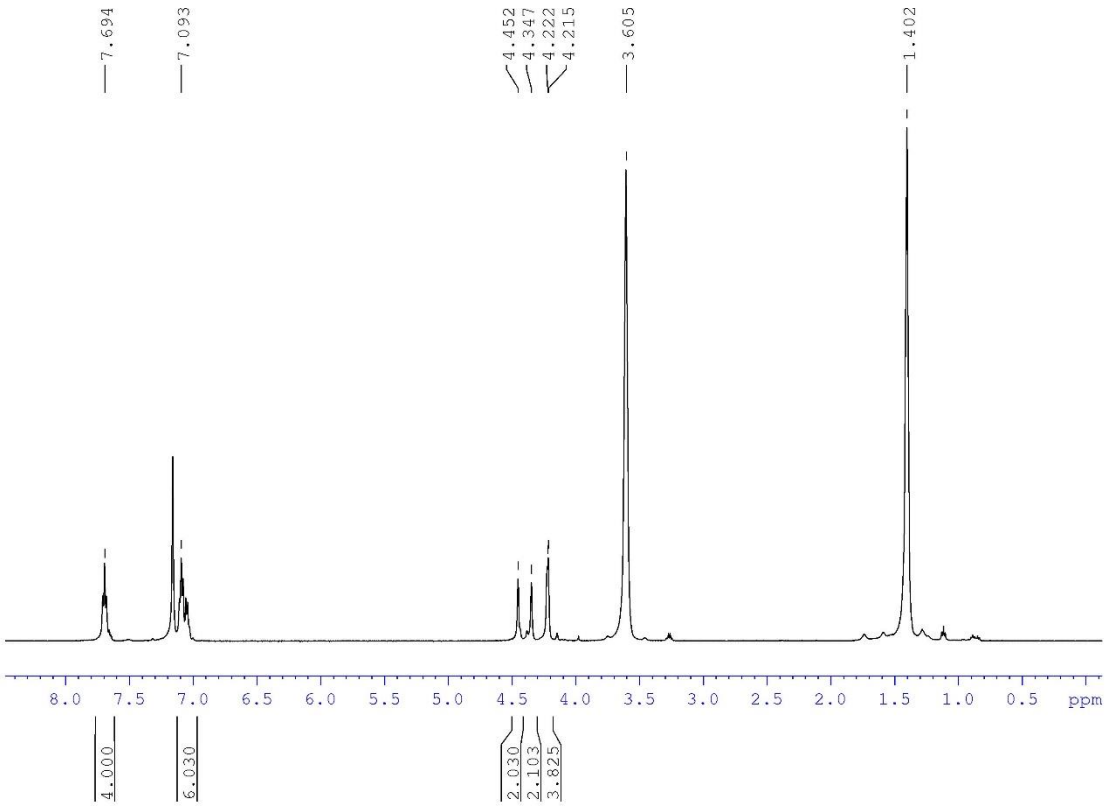

^{1}H NMR (500 MHz, C_6D_6) δ (ppm) 4.22 (t, 4H, Cp-H, J = 1.83 Hz), 4.35 (s, 2H, Cp-H), 4.45 (s, 2H, Cp-H), 7.09 (m, 6H, *m*-Ph, *p*-Ph), 7.69 (m, 4H, *o*-Ph); peaks at 1.40 and 3.61 were attributed to coordinated and residual diethyl ether.

[fc(PPh$_2$)(BH[(3,5-Me)$_2$pz]$_2$)][Li(THF)$_2$]

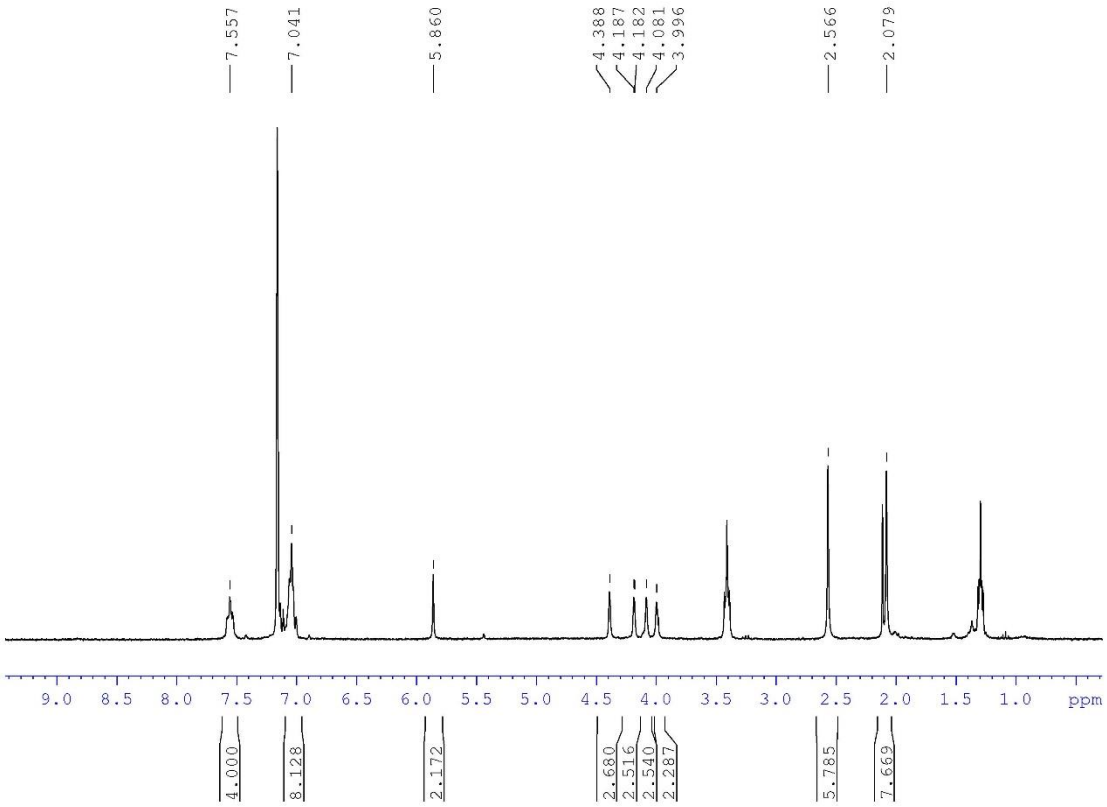

^{1}H NMR (300 MHz, C_6D_6) δ (ppm) 2.07 (s, 6H, -CH_3), 2.57 (s, 6H, -CH_3), 4.00 (t, 2H, Cp-H, J = 1.34 Hz), 4.08 (t, 2H, Cp-H, J = 1.55 Hz), 4.18 (t, 2H, Cp-H, J = 1.56 Hz), 4.39 (t, 2H, Cp-H, J = 1.84 Hz), 5.86 (s, 2H, -CH-), 7.04 (m, 6H, *m*-Ph, *p*-Ph), 7.56 (m, 4H, *o*-Ph); peaks at 1.29 and 3.45 were attributed to residual diethyl ether.

3-phenyl-5-methyl-1H-pyrazole

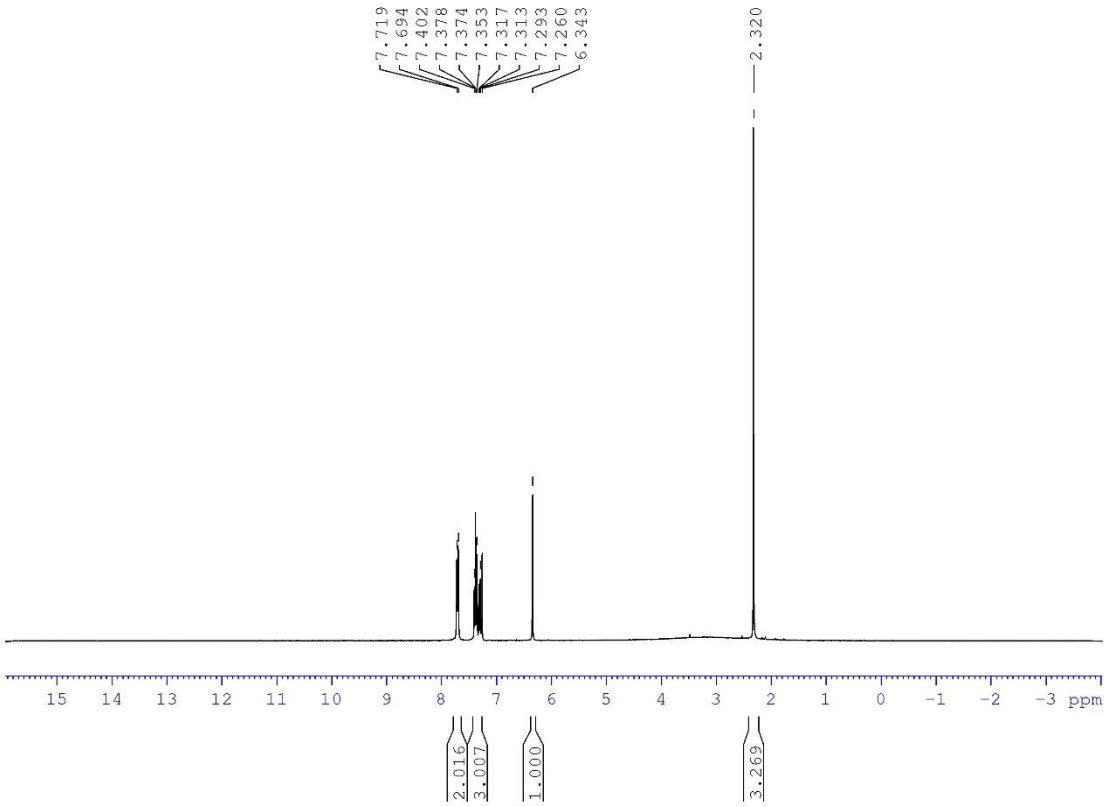

^{1}H NMR (300 MHz, $CDCl_3$) δ (ppm) 2.32 (s, 3H, -CH_3), 6.34 (s, 1H, -CH-), 7.31 (m, 3H, *m*-Ph, *p*-Ph), 7.70 (d, 2H, *o*-Ph, J = 7.46 Hz).

3,5-di-*tert*-butyl-1H-pyrazole

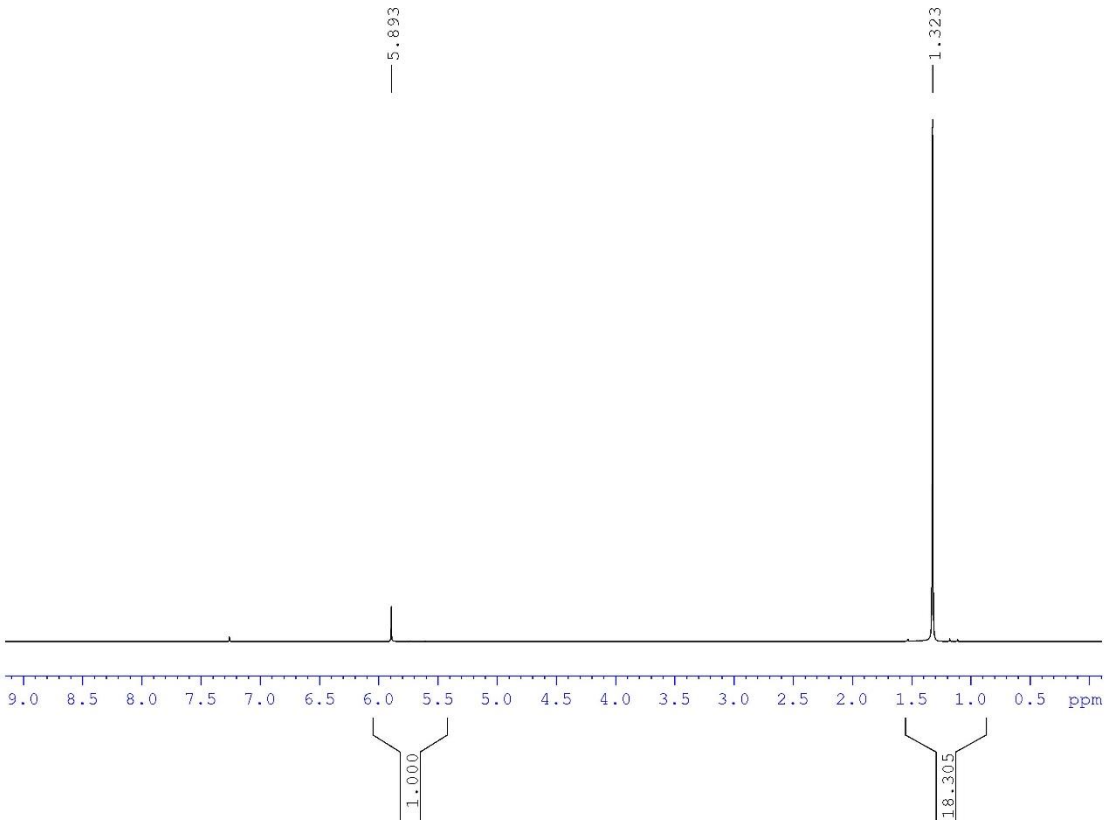

^{1}H NMR (300 MHz, $CDCl_3$) δ (ppm) 1.32 (s, 18H, -CH_3), 5.89 (s, 1H, -CH-).

[fc(PPh$_2$)(BH[(3,5-t-Bu)$_2$pz]$_2$)][Li(THF)$_2$] -- (NMR SCALE)

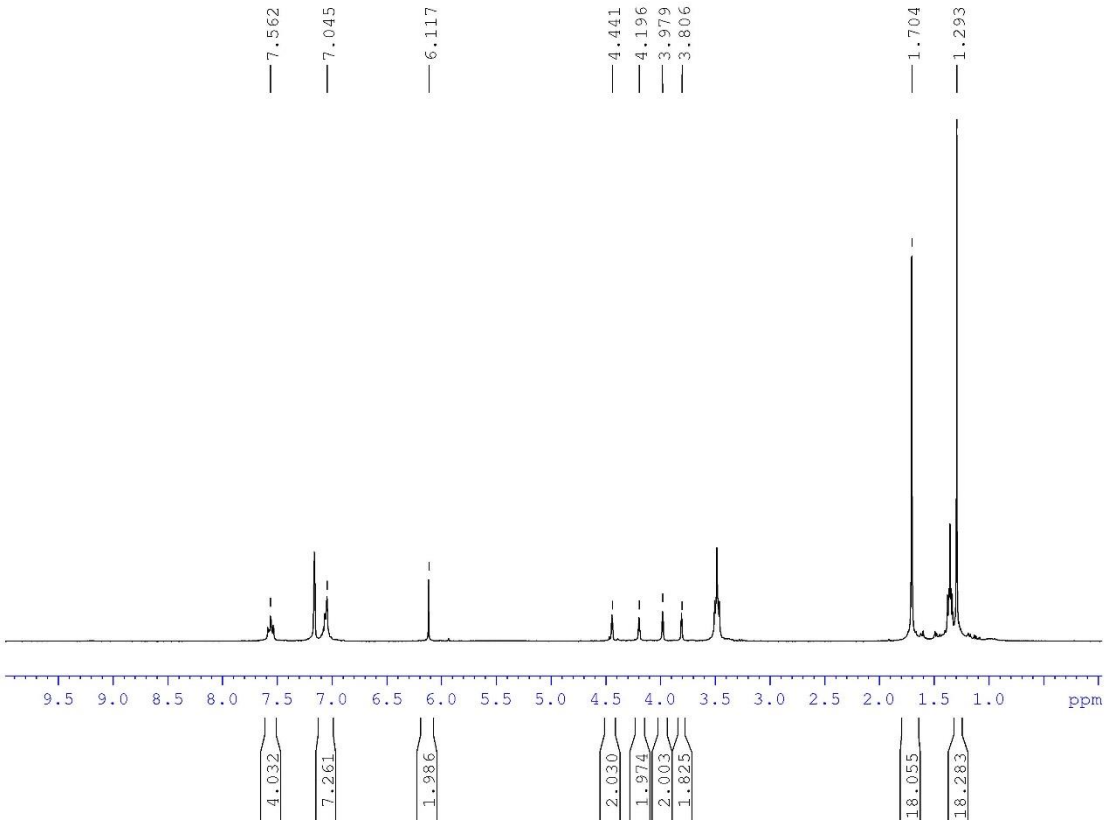

^{1}H NMR (300 MHz, C_6D_6). Successful only on sealed NMR scale. Heating up on a Schlenk line on larger scale leads to thermal decomposition of borohydride compound. See below for decomposition study.

($fc^{P,B}$)ZnCl

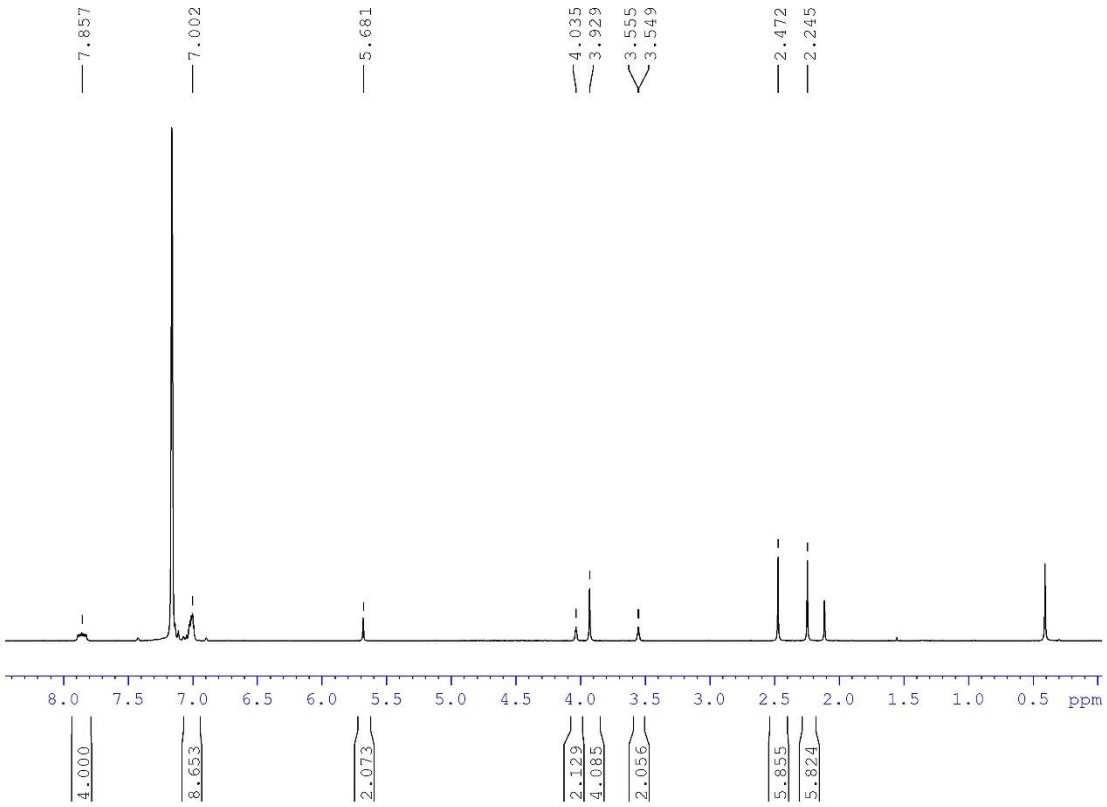

^{1}H NMR (300 MHz, C_6D_6) δ (ppm) 2.24 (s, 6H, -CH_3), 2.47 (s, 6H, -CH_3), 3.55 (t, 2H, Cp-H, 1.65 Hz), 3.93 (s, 4H, Cp-H), 4.03 (t, 2H, Cp-H, J = 1.79 Hz), 5.68 (s, 2H, -CH-), 7.00 (m, 6H, *m*-Ph, *p*-Ph), 7.86 (m, 4H, *o*-Ph); excess peaks are due to residual toluene.

[(fc^{P,B})Zn(μ-OCH$_2$Ph)]$_2$

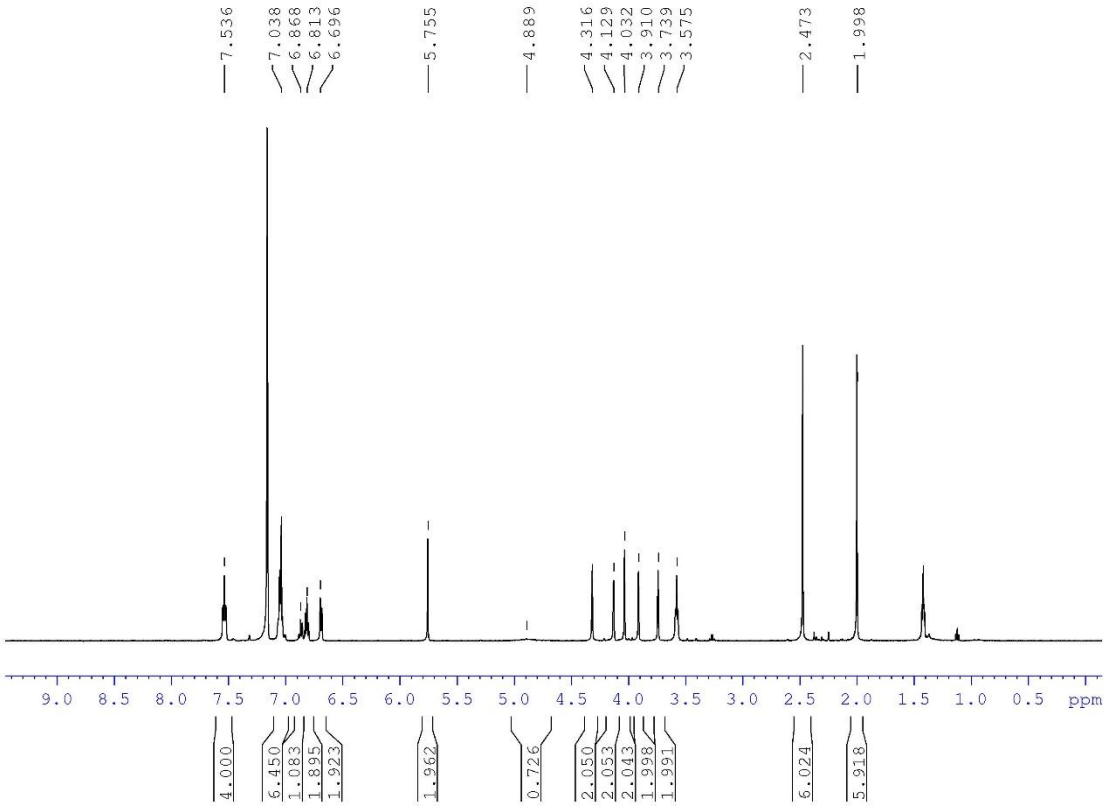

^{1}H NMR (500 MHz, C_6D_6) δ (ppm) 2.00 (s, 6H, -CH_3), 2.47 (s, 6H, -CH_3), 3.74 (t, 2H, Cp-H, J = 1.46 Hz), 3.91 (t, 2H, Cp-H, J = 1.24 Hz), 4.03 (s, 2H, -OCH_2Ph), 4.13 (t, 2H, Cp-H, J = 1.32 Hz), 4.31 (t, 2H, Cp-H, J = 1.27 Hz), 4.89 (s, 1H, BH), 5.75 (s, 2H, -CH-), 6.70 (m, 2H, *o*-Ph), 6.81 (m, 2H, *m*-Ph), 6.86 (m, 2H, *p*-Ph), 7.04 (m, 6H, *m*-Ph, *p*-Ph), 7.54 (m, 4H, *o*-Ph); residual diethyl ether and THF give rise to remaining peaks.

Polymerization of 1,2-Anhydro-3,4,6-tri-O-benzyl-α-d-glucopyranose

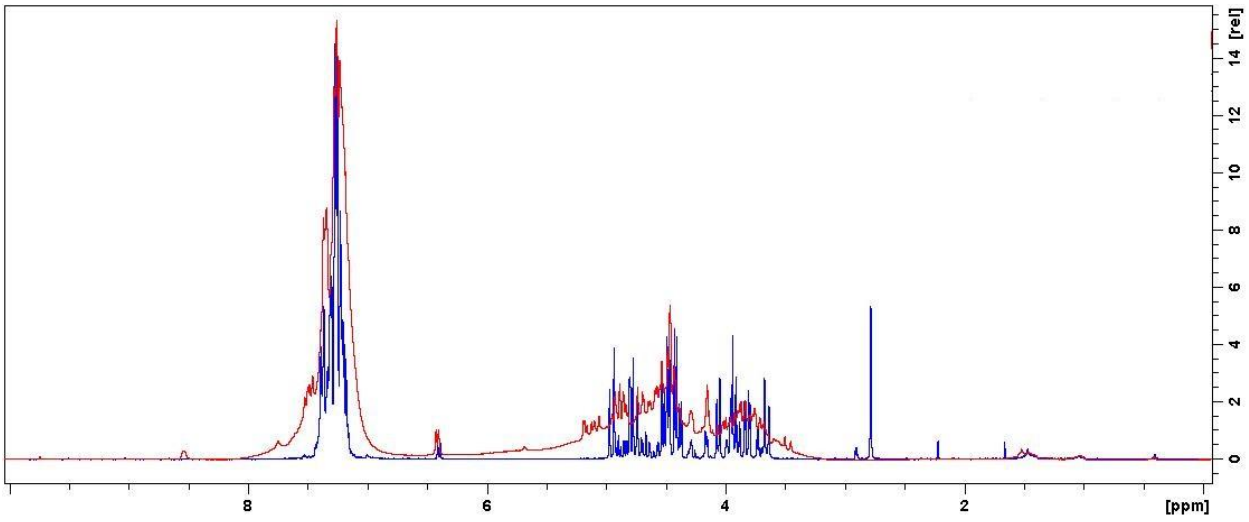

Blue is the before and red is the after. The characteristic formation of a ‘hill’ seen centered on 4.5 ppm is much like that observed in a norborene polymerization.

Attempted Synthesis of [fc(PPh_2)(BH[(3-Ph-5-Me)$_2$pz]$_2$)][Li(THF)$_2$]

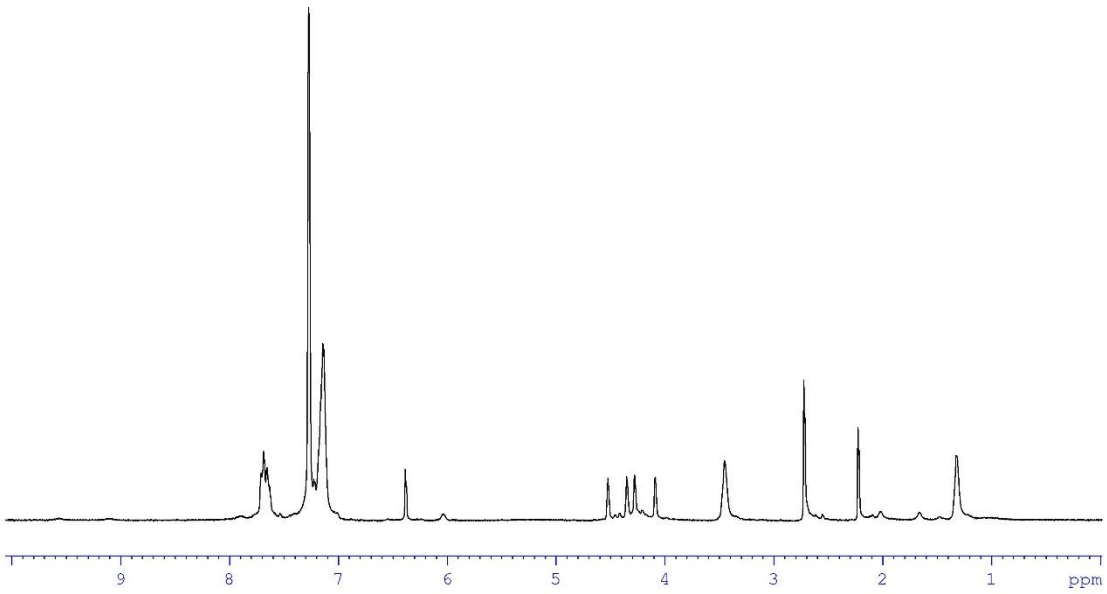

^{1}H NMR (300 MHz, C_6D_6). The formation of a cleaner product, seen here, was only attained through excess pyrazole addition, seen as bumps around 9 ppm and definitively at 6 ppm. The peaks formed with a broad base, and the ferrocene peaks integrated to show multiple compounds present. While this product looks clean, follow up with the zinc chloride reaction lead to messy NMR's and decomposition upon crystallization.

Thermal Decomposition

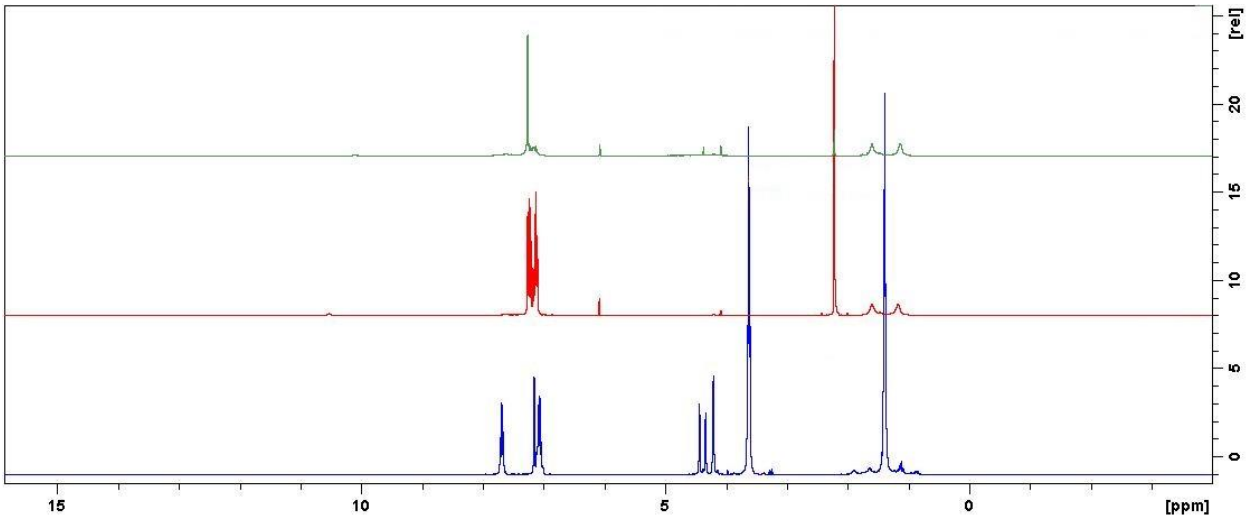

The borohydride compound [fc(PPh_2)(BH_3)][Li(OEt_2)] was heated up and studied for thermal decomposition. Blue is initial, Red is midpoint, Green is end result. Prolonged heating above 80°C decoordinates the lithium salt and destroys the complex.

References

1. Crabtree, R., *Organometallics*, **2011**, 30 (1), pp 17–19.
2. Wilkinson, G.; Rosenblum, M.; Whiting, M. C.; Woodward, R. B., *J. Am. Chem. Soc.* **1952,** 74 (8): 2125–2126.
3. Chirik, P. J., *J. Am. Chem. Soc*. **2009**, 131 (10), 3788–3789.
4. Ornelas, C., *New J. Chem*., **2011**, 35, 1973-1985.
5. Engtrakul, C.; Sita, L., *Nano Letters*, **2001**, 1 (10), pp 541–549.
6. Rausch, M.; Fischer, E.; Grubert, H., *J. Am. Chem. Soc.*, **1960**, 82 (1), pp 76–82.
7. Sampson, J.; Choi, G.; Akhtar, M.; Jaseer, E.; Theravalappil, R.; Al-Mualem, H.; Agapie, T., *Organometallics*, **2017**, 36 (10), pp 1915–1928.
8. Brintzinger, H.; Fischer, D.; Mulhaupt, R.; Rieger, B.; Waymouth, R., *Angew. Chem. Int. Ed. Engl.* **1995**. 34, 1143.
9. Abubekerov, A.; Khan, S.; Diaconescu, P., *Organometallics*, **2017**, 36 (22), pp 4394–4402
10. Silva, M.; Pombeiro, A.; Fraústo da Silva, J.; Herrmann, R.; Deus, N.; Bozak, R., *Journal of Organometallic Chemistry*, **1994**, 480, 1–2, 81-90.
11. Gregson, C. K. A.; Gibson, V. C.; Long, N. J.; Marshall, E. L.; Oxford, P. J.; White, A. J. P., *J. Am. Chem. Soc.* **2006**, *128* (23), 7410–7411.
12. Quan, Stephanie M.; Wei, Junnian; Diaconescu, Paula L., *Organometallics* **2017**, *36 (22)*, 4451-4457.
13. Anderson Jr., W; Long, B., *ACS Macro Lett.*, **2016**, 5 (9), pp 1029–1033.
14. Quan, S.; Wang, X.; Zhang, R.; Diaconescu, P., *Macromolecules*, **2016**, 49 (18), pp 6768–6778.
15. Trofimenko, S., *J. Am. Chem. Soc.* **1966,** *88*, 1842.

16. 2. Trofimenko, S., *Chem. Rev.* **1993,** *93*, 943.

17. 3. Trofimenko, S., *J. Chem. Ed.* **2005,** *82*, 1715.

18. Pavlovic, M.; Stepanovic, S.; Peric, M.; Guell, M.; Swart, M., *Phys. Chem. Chem. Phys.*, **2014**,16, 14514-14522

19. Hikichi, S.; Hanaue, K.; Fujimura, T.; Okuda, H.; Nakazawa, J.; Ohzu, Y.; Kobayashi, C.; Akita, M., *Dalton Trans.* **2013,** *42*, 3346.

20. Dias, H. V. R.; Lovely, C. J., *Chem. Rev.* **2008,** *108*, 3223.

21. Caballero, A.; Despagnet-Ayoub, E.; Mar Díaz-Requejo, M.; Díaz-Rodríguez, A.; González-Núñez, M. E.; Mello, R.; Muñoz, B. K.; Ojo, W.-S.; Asensio, G.; Etienne, M.; Pérez, P. J., *Science* **2011**, 332, 835.

22. Lu, Z.; Williams, T. J., *Chem. Commun.* **2014**, 50, 5391.

23. Fraser, L. R.; Bird, J.; Wu, Q.; Cao, C.; Patrick, B. O.; Love, J. A., *Organometallics* **2007**, 26, 5602.

24. Momin, A.; Bonnet, F.; Visseaux, M.; Maron, L.; Takats, J.; Ferguson, M. J.; Le Goff, X.-F.; Nief, F., *Chem. Commun.* **2011**, 47, 12203.

25. Pettinari, C.; Marchetti, F.; Cerquetella, A.; Pettinari, R.; Monari, M.; Mac Leod, T. C. O.; Martins, L. s. M. D. R. S.; Pombeiro, A. J. L., *Organometallics* **2011**, 30, 1616.

26. Cao, C.; Fraser, L. R.; Love, J. A., *J. Am. Chem. Soc.* **2005**, 127, 17614.

27. Ilkhechi, A. H.; Bolte, M.; Lerner, H.-W.; Wagner, M., *J. Organomet. Chem*. **2005**, 690, 1971.

28. Herdtweck, E.; Peters, F.; Scherer, W.; Wagner, M., *Polyhedron* **1998**, 17, 1149.

29. Jäkle, F.; Polborn, K.; Wagner, M., *Chem. Ber*. **1996**, 129, 603.

30. Guo, S.; Peters, F.; Fabrizi de Biani, F.; Bats, J. W.; Herdtweck, E.; Zanello, P.; Wagner, M., *Inorg. Chem*. **2001**, 40, 4928.

31. Sirianni, E. R.; Yap, G. P. A.; Theopold, K. H., *Inorg. Chem*. **2014**, 53, 9424.

32. Fabrizi de Biani, F.; Jäkle, F.; Spiegler, M.; Wagner, M.; Zanello, P., *Inorg. Chem.* **1997**, 36, 2103.

33. Sanford, M.; Love, J.; Grubbs, R., *J. Am. Chem. Soc.*, **2001**, 123 (27), pp 6543–6554.

34. Tolman, C.; *Chem. Rev.*, **1977**, 77 (3), pp 313–348.

35. Laly, M.; Broussier, R.; Gautheron, B., *Tetrahedron Letters*, **2000**, 41, 8, 1183-1185.

36. Pangborn, A. B.; Giardello, M. A.; Grubbs, R. H.; Rosen, R. K.; Timmers, F. J., *Organometallics,* **1996**,15, 1518.

37. Bishop, J. J.; Davison, A.; Katcher, M. L.; Lichtenberg, D. W.; Merrill, R. E.; Smart, J. C. J. *Organomet. Chem.* **1971**, 27, 241.

38. Shafir, A.; Power, M. P.; Whitener, G. D.; J. Arnold. *Organometallics,* **2000**, 19, 3978–3982.

39. Butler, I. R.; Davies, R. L. *Synthesis* **1996**, 1350.

40. Abubekerov, M.; Diaconescu, P.; *Inorganic Chemistry*, **2015**. 54(4), pp.1778-1784.

41. Govindaswamy, P.; Mozharivskyj, Y.; Kollipara, M.; *Journal of Organometallic Chemistry*, **2004**, 689(20), 3265-3274.

42. Van Wyk, J.; Omondi, B.; Appavoo, D.; Guzei, I.; Darkwa, J.; *Journal of Chemical Research*, **2012**, 36(8), 474-477.

43. Enthaler, S., *ACS Catal.*, **2013**, 3 (2), 150–158

44. Kernbichl, S.; Reiter, M.; Adams, F.; Vagin, S.; Rieger, B., *J. Am. Chem. Soc.*, **2017**, 139 (20), 6787–6790.

45. Abubekerov, M.; Wei, J.; Swartz, K.; Xie, Z.; Pei, Q.; Diaconescu, P., *Chem. Sci.*, **2018**, 9, 2168-2178.

46. Osten, K.; Mehrkhodavandi, P., *Acc. Chem. Res.*, **2017**, 50 (11), 2861–2869.

47. Cheshev, P.; Marra, A.; Dondoni, A., *Carbohydrate Research*, **2006**, 341, 16, 2714-2716.

48. Aguilar-Parrilla, F.; Cativiela, C.; Diaz de Villegas, M.; Elguero, J.; Foces-Foces, C.; Laureiro, J.; Cano, F.; Limbach, H.; Smith, J.; Toiron, C., *J. Chem. Soc., Perkin Trans*., **1992**, 2, 1737-1742.